Stable isotope patterns of mesopelagic communities over two shallow seamounts of the south-western Indian Ocean

Annasawmy Pavanee [1, 2, *], Cherel Yves [3], Romanov Evgeny V. [4], Le Loch Francois [5], Ménard Frédéric [6], Ternon Jean-Francois [1], Marsac Francis [1, 2]

[1] MARBEC, IRD, Univ Montpellier, CNRS, Ifremer, Sète, France
[2] Department of Biological Sciences and Marine Research Institute/ICEMASA, University of Cape Town, Cape Town, South Africa
[3] Centre d'Etudes Biologiques de Chizé (CEBC), UMR7372 du CNRS- La Rochelle Université, Villiers-en-Bois, France
[4] Centre technique d'appui à la pêche réunionnaise (CAP RUN - CITEB), Île de la Réunion, France
[5] IRD, Univ Brest, CNRS, Ifremer, LEMAR, IUEM, F-29280, Plouzane, France
[6] Aix Marseille Univ, Université de Toulon, CNRS, IRD, MIO, UM110, Marseille, France

* Corresponding author : Pavanee Annasawmy, email address : angelee-pavanee.annasawmy@ird.fr

Abstract :

The stable carbon ($\delta^{13}C$) and nitrogen ($\delta^{15}N$) isotope values of soft tissues of micronekton (crustaceans, squid, mesopelagic fish) and zooplankton were measured from organisms collected on the RV Antea at two seamounts located in the south-western Indian Ocean: La Pérouse (summit depth ~60 m) and "MAD-Ridge" (thus named in this study; summit depth ~240 m). Surface particulate organic matter (POM-Surf) showed higher $\delta^{13}C$ at the more productive MAD-Ridge than at the oligotrophic La Pérouse seamount. Particulate organic matter and zooplankton were depleted in 15N at La Pérouse pinnacle compared with MAD-Ridge. Gelatinous organisms and crustaceans occupied the lowest and intermediate trophic levels (TL ~2 and 3 respectively) at both seamounts. Mesopelagic fish and smaller-sized squid sampled at both seamounts occupied TL ~3 to 4, whereas the large nektonic squid, Ommastrephes bartramii, collected at MAD-Ridge only, exhibited a TL of ~5. The $\delta^{15}N$ values of common open-water mesopelagic taxa were strongly influenced by specimen size and feeding habits at both seamounts, with an increase in $\delta^{15}N$ values with increasing size. Carnivorous fish species sampled exclusively over the seamounts' flanks and summits exhibited TL values of ~4, irrespective of their wide size ranges. The work could not demonstrate any differences in $\delta^{15}N$ values of mesopelagic fish between the seamounts and the surrounding oceanic areas. The study segregated clusters of mesopelagic organisms according to their $\delta^{13}C$ and $\delta^{15}N$ values, with variations in stable isotope values reflecting a complex range of processes possibly linked to productivity as well as biological and ecological traits of the species (size and feeding mode).

Keywords : micronekton, crustaceans, fish, $\delta^{13}C$, $\delta^{15}N$, trophic level

1. Introduction

Micronekton are a broad group of organisms mostly dwelling in the mesopelagic zone (<1000 m). They consist of crustaceans (adult euphausiids, hyperiid amphipods, pelagic decapods and mysids), cephalopods (small species and juvenile stages of large oceanic species) and fish (mainly mesopelagic species and juveniles of pelagic fish) (Brodeur & Yamamura, 2005; De Forest & Drazen, 2009; Ménard et al., 2014). They range in size from 2 to 20 cm and represent a substantial biomass in oceanic waters (Brodeur & Yamamura, 2005). Many species exhibit extensive diel vertical migrations (DVM), thus playing an important role in the biological pump by transporting carbon and nutrients from the epipelagic to the mesopelagic zone (Hidaka et al., 2001; Brodeur & Yamamura, 2005; Catul et al., 2011; Bianchi et al., 2013). Micronekton also form a key trophic link between zooplankton and top predators because they are preyed upon by several species of seabird, tuna and billfish (Guinet et al., 1996; Bertrand et al., 2002; Brodeur & Yamamura, 2005; Potier et al., 2007; Karakulak et al., 2009; Cherel et al., 2010; Danckwerts et al., 2014; Jaquemet et al., 2014; Duffy et al., 2017; Watanuki & Thiebot, 2018). Various studies have investigated the trophic interactions of micronekton to better understand their role in foodwebs across numerous ocean basins (Fanelli et al., 2011b; Colaço et al., 2013; Fanelli et al., 2013; Ménard et al., 2014; Valls et al.., 2014a, b; Annasawmy et al., 2018). For instance, mesopelagic organisms were shown to transfer energy between primary consumers and deeper benthic and benthopelagic animals at Condor seamount in the Atlantic (Colaço et al., 2013).

Tuna, billfish, pelagic armorheads, alfonsinos and orange roughy are common predators fished extensively at seamounts in the Atlantic (Fonteneau, 1991; Morato et al., 2008; Dubroca et al., 2013), Pacific (Rogers, 1994; Koslow, 1997; Holland et al., 1999; Musyl et al., 2003; Paya et al., 2006; Morato et al., 2010) and Indian oceans (Romanov, 2003; Clark et

26 al., 2007; Marsac et al., 2014). Although, La Pérouse does not represent an outstanding

27 fishing spot, tuna (*Thunnus* spp.) and swordfish (*Xiphias gladius*) are present in the vicinity

28 of the seamount throughout the year (Marsac et al., 2020). Albacore (*Thunnus alalunga*),

29 bigeye (*T. obesus*), yellowfin (*T. albacares*) tuna and swordfish commonly occur along the

30 Madagascar Ridge and MAD-Ridge pinnacle (IOTC, www.iotc.org/data-and-statistics). The

31 Madagascar Ridge has also been targeted for orange roughy in 1999/2000 before the catch

32 dropped significantly in subsequent years (Ingole & Koslow, 2005; Lack et al., 2003). Due to

33 the increased pressure on marine organisms, characterizing the overall energy flow within

34 pelagic ecosystems (Young et al., 2015) contributes to making better informed fisheries and

35 ecosystem-based management decisions.

36 Two seamounts of the southwestern Indian Ocean (SWIO), La Pérouse and an unnamed

37 pinnacle, thereafter named "MAD-Ridge", were studied in an effort to understand how

38 seamounts may affect diel vertical migrations and aggregations of micronekton (Annasawmy

39 et al., 2019, 2020). While micronekton acoustic densities were not significantly different

40 between the summit and immediate vicinity of the pinnacles, dense aggregations of scatterers,

41 referred to as seamount-associated species, were recorded over the summit of both seamounts

42 during day and night (Annasawmy et al., 2019). La Pérouse is situated in the Indian South

43 Subtropical Gyre (ISSG) province (Longhurst, 2007; Reygondeau et al., 2013) with low

44 mesoscale activities and primary productivity, whereas MAD-Ridge is located within an

45 "eddy corridor" to the south of Madagascar, in a region with high occurrence of cyclonic and

46 anticyclonic eddies and relatively high sea surface chlorophyll concentrations all year round

47 compared to La Pérouse (Halo et al., 2014; Annasawmy et al., 2019; Vianello et al., 2020).

48 The enhanced productivity on the Madagascar shelf and its offshore entrainment by

49 mesoscale eddy interactions (Quartly et al., 2006), were one possible reasons leading to

50 greater micronekton acoustic densities at MAD-Ridge relative to La Pérouse (Annasawmy et

4

51 al., 2020). Trapped, enclosed circulations known as Taylor columns may also develop over

52 seamounts and contribute to the retention of productivity (Genin & Boehlert, 1985; Dower et

53 al., 1992; Mouriño et al., 2001; Mohn & White, 2007). No Taylor columns were observed at

54 La Pérouse and MAD-Ridge seamounts, however, during the cruises most likely because of

55 the high current speeds observed over the summits and the seamount structure not being

56 favourable for the development and retention of such features (Annasawmy et al., 2020).

57 Foodwebs are shaped by a complex set of interactions controlled by the availability of

58 organic (C-based nutrients) and inorganic (such as nitrate, nitrite, phosphate and silicate)

59 nutrients, the efficiency of energy transfer to higher trophic levels and the control of species

60 biomass by predators (Pomeroy, 2001). Carbon ($\delta^{13}C$) and nitrogen ($\delta^{15}N$) stable isotope

61 analyses are a valuable tool for foodweb investigations in deep-sea ecosystems (Michener &

62 Kaufman, 2007) and are based on time-integrated assimilated food (Martínez del Rio et al.,

63 2009). Trophodynamic studies commonly employ $\delta^{13}C$ to investigate the source of organic

64 matter and $\delta^{15}N$ to determine trophic level and trophic interactions (Michener & Kaufman,

65 2007). The heavier isotopes (^{13}C and ^{15}N) are preferentially retained in tissues of consumers

66 relative to their prey, while lighter ^{12}C and ^{14}N isotopes are preferentially excreted (Fry,

67 2006). Overall, there is a small isotopic enrichment of 0.5-1‰ in the heavier ^{13}C isotope of

68 an organism's tissue relative to its diet (Fry, 2006). Differences in $\delta^{13}C$ values can thus

69 indicate different sources of primary production such as inshore vs offshore, or pelagic vs

70 benthic contributions to food intake (Hobson et al., 1994; Rubenstein & Hobson, 2004). In

71 contrast, $\delta^{15}N$ values increase stepwise by 2-4‰ in a consumer's tissue relative to its diet

72 (Vanderklift & Ponsard, 2003; Michener & Kaufman, 2007; Martínez Del Rio et al., 2009),

73 thus allowing the discrimination of trophic levels.

74 Identification of the trophic position of various biotic components of the pelagic ecosystem is

75 essential for our understanding of ecosystem functioning and trophic interactions. Food chain

76 length (i.e. number of TLs) is a descriptor of community structure and ecosystem functioning

77 (Post et al., 2000). Measuring the length of a food chain integrates the assimilation of energy

78 flow through all trophic pathways leading to top predators. The understanding of this is

79 essential from an ecosystem-based management perspective, and may provide important

80 insights on ecosystem responses to fisheries- pressure and/or climate-induced changes.

81 Knowledge of micronekton trophic interactions at seamount ecosystems of the SWIO are

82 scarce and fragmentary. In order to investigate the trophic pathways at La Pérouse and MAD-

83 Ridge, δ^{13}C and δ^{15}N values of POM, zooplankton and micronekton were measured and

84 trophic levels were estimated using additive isotopic models (as in Post, 2002, and Caut et al.,

85 2009). The main goals of this study were to investigate at La Pérouse and MAD-Ridge

86 seamounts, (1) the trophic interactions of sampled mesopelagic organisms, (2) the influence

87 of trophic groups, specimen size and time of sampling (MAD-Ridge only) on δ^{13}C and δ^{15}N

88 values of micronekton, (3) the δ^{13}C and δ^{15}N values of omnivorous/carnivorous fish collected

89 over the flank relative to the vicinity of La Pérouse; and summit, flanks and vicinity of MAD-

90 Ridge compared with an off-seamount location in the southern Mozambique Channel.

91

92 **2. Material and methods**

93 2.1 Study sites

94 2.1.1 La Pérouse seamount

95 La Pérouse is located on the outskirts of the oligotrophic ISSG province (Longhurst, 1998,

96 2007; Reygondeau et al., 2013), 160 km northwest of Réunion Island at latitude 19°43'S and

97 longitude 54°10'E (Fig. 1a, b). The seamount summit reaches the euphotic zone, being ~60 m

98 below the sea surface. The summit is 10 km long with narrow and steep flanks and rises from

6

99   a depth of 5000 m from the ocean floor. The pinnacle was sampled on board the RV *Antea*

100   from 15 to 29 September 2016 (DOI: 10.17600/16004500).

101   2.1.2 MAD-Ridge seamount

102   This topographic feature, located ~240 km to the south of Madagascar, along the Madagascar

103   Ridge at latitude 27°29'S and longitude 46°16'E has been named "MAD-Ridge" in this study

104   (Fig. 1a, c). The seamount rises from a depth of 1600 m from the ocean floor to ~240 m

105   below the sea surface. The summit is 33 km long (north to south) and 22 km wide (east to

106   west). MAD-Ridge is surrounded by four smaller pinnacles, reaching depths of 600 m, 900

107   m, 800 m and 1200 m below the sea surface, between latitudes 27°S-28°S and longitudes

108   46°E-46°45'E. The MAD-Ridge pinnacle was sampled on board the RV *Antea* (DOI:

109   10.17600/16004800 and 10.17600/16004900) from 26 November to 14 December 2016.

110   2.2 Satellite observations

111   Sea surface chlorophyll data were downloaded from the MODIS dataset

112   (http://oceancolor.gsfc.nasa.gov) at a daily and 4.5 km resolution. Five-day averages were

113   calculated to obtain a proxy of phytoplankton abundance in the surface layer. To investigate

114   the annual variability in surface chlorophyll *a* concentrations, monthly mean concentrations

115   were averaged from January to December 2016 for the defined regions (La Perouse: 18.5-

116   20°S/53-33°E; MAD-Ridge: 27-28°S/44-48°E) (Fig. 2).

117   2.3 Sampling and sample processing

118   2.3.1 Particulate organic matter (POM)

119   During both cruises, water samples for stable isotope analyses of POM were collected using

120   Niskin bottles mounted on a Sea-Bird 911 + CTD rosette system at approximately 5 m depth

121   (referred to as POM-Surf) and at the depth of maximum fluorescence (referred to as POM-

122 Fmax) between ~60 and 125 m at La Pérouse and ~80 and 150 m at MAD-Ridge. Between 4

123 and 8 l (depending on the load of each sample) of seawater were filtered on precombusted 25

124 or 47 mm glassfibre of 0.7 µm pore size. The filters were oven-dried at 50°C for 24 h and

125 saved at room temperature in aluminium foil until further analyses.

126 2.3.2 Zooplankton sampling

127 Zooplankton samples were collected during daylight only with a Bongo net (300 µm mesh to

128 a maximum depth of 500 m and 200 µm mesh to a maximum depth of ~200 m) towed

129 obliquely at La Pérouse (10 stations). At MAD-Ridge, zooplankton samples were also

130 collected during daylight with a Bongo net (300 µm mesh to a maximum depth of 500 m

131 towed obliquely and 63 µm mesh to the depth of the maximum fluorescence towed vertically)

132 at 19 stations. The nets were fitted with a flowmeter and were towed at a vessel speed of 1.5-

133 2 knots for 15-20 min (0.28 m^2 mouth area). Zooplankton samples from the 200 and 300 µm

134 meshes at La Pérouse and, from the 63 and 300 µm meshes at MAD-Ridge were combined at

135 each station. The combined samples at each station were sieved on a stack of seven sieves of

136 decreasing mesh size and divided into six fractions: >4000 µm, 4000-2000 µm, 2000-1000

137 µm, 1000-500 µm, 500-250 µm, 250-125 µm during La Pérouse and MAD-Ridge and a 7th

138 fraction (125-63 µm) during MAD-Ridge only. Each fraction was oven-dried at 50°C for 24 h

139 and frozen on board at -20°C before being analysed for stable isotope analyses (section 2.4).

140 Zooplankton abundances, biomasses and taxa composition at the seamounts and off-

141 seamount locations are investigated in Noyon et al. (2020).

142 2.3.3 Trawl sampling

143 During both cruises, a 40-m long International Young Gadoid Pelagic Trawl (IYGPT) net

144 (codend with 0.5 cm knotless nylon delta mesh; front tapering end with 8 cm mesh; ~96 m^2

145 mouth opening) was towed at a vessel speed of 2-3 knots for 60 mins during La Pérouse and

146   for 30 min during MAD-Ridge to sample mesopelagic organisms. Trawls were carried out in

147   the shallow (0-200 m), intermediate (200-400 m) and deep (below 400 m) layers during both

148   cruises (Supplementary Material, Table 1). Trawl stations at La Pérouse and MAD-Ridge

149   (Fig. 1b, c) were further classified into the categories summit, flank and vicinity- according to

150   whether they occurred on the summit plateau of the seamounts, along the flanks (seafloor

151   depth of 300-1300 m) or in the immediate vicinity (depth >1300 m) (Supplementary

152   Material, Table 1). Four other mesopelagic trawls (#18-21) were conducted in the southern

153   Mozambique Channel (depth >4000 m) during the MAD-Ridge cruise as reference stations

154   for non-seamount locations within the EAFR province (Fig. 1a).

155   All organisms collected with the trawl were sorted on board, divided into four broad

156   categories (gelatinous, crustaceans, cephalopods and fish), counted and identified to the

157   lowest possible taxon. Individuals from these four broad categories were randomly selected

158   according to their occurrence and abundance and measured (total length for selected

159   gelatinous organisms, abdomen and carapace length for selected crustaceans, dorsal mantle

160   length for cephalopods and standard length for fish). Approximately 2 to 5 mg of soft tissues

161   of these selected individuals (muscle tissue for leptocephali, muscle abdomen for crustaceans,

162   mantles for squid, dorsal muscle for fish) and whole salps and pyrosomes, were sampled on

163   board in 2 ml Eppendorf tubes and stored at -20°C, before being processed in the laboratory

164   to determine $\delta^{13}C$ and $\delta^{15}N$ values (section 2.4). A list of selected gelatinous and micronekton

165   taxa used in stable isotope analyses is given in Supplementary Material, Table 2.

166   2.4 Stable isotope analysis

167   Micronekton and zooplankton samples were freeze-dried using Christ Alpha 1-4 LSC freeze-

168   dryers for 48 h and ground to a fine homogeneous powder using an automatic ball mill

169   RETSCH MM200. As variations in lipid composition may influence $\delta^{13}C$ and $\delta^{15}N$ values

170 (Bodin et al., 2009; Ryan et al., 2012), lipids were removed from zooplankton and

171 micronekton samples with dichloromethane on an accelerated solvent extraction system

172 (ASE®, Dionex; Bodin et al., 2009). Prior to δ^{13}C analyses, POM filters and zooplankton

173 samples were reacted with 1 N HCl to remove carbonates (Cresson et al., 2012). Untreated

174 subsamples of POM and zooplankton were used to measure δ^{15}N because acid treatment may

175 lead to the loss of nitrogenous compounds (Kolasinski et al., 2008). POM filters were cut,

176 folded and put into tin capsules. Approximately 400-600 µg of each zooplankton and

177 micronekton sample were weighed and placed in tin capsules. These samples were run

178 through continuous flow on a Thermo Scientific Flash EA 2000 elemental analyser coupled

179 to a Delta V Plus mass spectrometer at the Pôle de Spectrométrie Océan (Plouzané, France).

180 The samples were combusted in the elemental analyser to separate CO_2 and N_2. A reference

181 gas set was used to determine isotopic ratios by comparison. The isotopic ratios are expressed

182 in the conventional δ notations as parts per thousand (‰) deviations from the international

183 standards:

184 δ^{13}C or δ^{15}N (‰) = [(R$_{sample}$/R$_{standard}$) − 1] x 1000

185 where R is the ratio of ^{13}C/^{12}C or ^{15}N/^{14}N.

186 2.5 Data analyses

187 2.5.1 Overall δ^{13}C and δ^{15}N signatures

188 Shapiro-Wilk and Bartlett tests were computed to test for assumptions of normality and

189 homogeneity of variances. Links between δ^{13}C and δ^{15}N values and the foodweb components

190 (POM-Surf, POM-Fmax, zooplankton, gelatinous organisms, crustaceans, squid and fish),

191 were investigated using Kruskal-Wallis (KW) tests and pairwise comparisons in R (version

192 3.3.1) because the data did not follow normal distributions. Kruskal-Wallis tests and pairwise

193 comparisons were also computed to investigate whether there was a significant difference in

194 $\delta^{13}C$ and $\delta^{15}N$ values for each foodweb component between La Pérouse and MAD-Ridge. To

195 assess the association between $\delta^{13}C$ and $\delta^{15}N$ values, Spearman rank correlation coefficients

196 were calculated with all foodweb components at each seamount. Wilcoxon rank sum tests

197 investigated the effect of time (day or night) on $\delta^{13}C$ and $\delta^{15}N$ values of gelatinous plankton

198 and micronekton at MAD-Ridge only (because a single daylight trawl was conducted at La

199 Pérouse and too few species were caught). To test for the effect of trawl position with respect

200 to the seamounts on $\delta^{13}C$ and $\delta^{15}N$ values of omnivorous/carnivorous fish, Wilcoxon Rank

201 sum tests and KW tests were performed on the La Pérouse and MAD-Ridge datasets,

202 respectively.

203 2.5.2 Layman community-wide metrics

204 The Layman community-wide metrics SEA_c and the $\delta^{13}C$ and $\delta^{15}N$ ranges (Layman et al.,

205 2007) were calculated using the SIBER package (version 2.1.4, Jackson et al., 2011). The

206 SEA_c (sample-size-corrected standard ellipse area) describes the overall extent of the isotopic

207 niches. The SEA_c is robust for sample sizes >10 (Daly et al., 2013), which is the case for all

208 the broad categories within this study. The SEA_c of each foodweb component was described

209 in terms of the space occupied by the group on a $\delta^{15}N$-$\delta^{13}C$ plot based on all the individuals

210 sampled within the group. The $\delta^{13}C$ and $\delta^{15}N$ ranges were used to describe and compare the

211 overall extents of the foodwebs at the La Pérouse and MAD-Ridge sites. Increased $\delta^{13}C$ range

212 would be expected in foodwebs with multiple basal sources with varying $\delta^{13}C$ values

213 suggesting niche diversification at the base of the foodweb, whereas the $\delta^{15}N$ range describes

214 the sampled food chain lengths (Portail et al., 2016).

215 2.5.3 Trophic level estimations

216 Different models have been applied across several studies to estimate the trophic level of

217 organisms: additive model with a fixed enrichment factor, additive enrichment model with a

218 variable isotopic enrichment or scaled model with decreasing isotopic enrichment factors

219 (Minagawa & Wada, 1984; Post, 2002; Caut et al., 2009; Hussey et al., 2014). Ménard et al.

220 (2014) and Annasawmy et al. (2018) used a fixed enrichment factor of 3.2‰ to estimate

221 trophic levels of foodweb components POM, zooplankton, gelatinous plankton and

222 micronekton collected in the SWIO. In this study, two alternative trophic enrichment

223 assumptions were compared to estimate the trophic level of all the measured individuals

224 within the groups (zooplankton, gelatinous organisms, crustaceans, squid and fish) at La

225 Pérouse and MAD-Ridge.

226 The TPA model (additive model with constant isotopic enrichment) was proposed by

227 Minagawa & Wada (1984) and Post (2002) with the reference level set at a trophic level of 2

228 for the primary consumer and a fixed and additive enrichment factor of 3.2‰:

229 Trophic level, $TPA = 2.0 + \frac{\delta^{15}N_i - \delta^{15}N_{primary\ consumer}}{3.2}$ Eq. 1

230 where, $\delta^{15}N_i$ the nitrogen isotopic composition of any given micronekton taxon i, $\delta^{15}N_{primary}$

231 $_{consumer}$ the $\delta^{15}N$ reference baseline value at trophic level 2, and 3.2‰ is an estimate of the

232 trophic enrichment factor between consumers and their primary prey (Michener & Kaufman,

233 2007; Vanderklift & Ponsard, 2003). The $\delta^{15}N$ values of POM, primary consumers and

234 zooplankton have been used in trophic level calculations as isotopic baseline (e.g. Lorrain et

235 al., 2015). Primary consumers are generally used as baseline to reduce errors in estimations

236 (Martínez Del Rio et al., 2009). Salps are known filter feeders which have been used as

237 baseline in previous studies in the region (Ménard et al., 2014). At La Pérouse, the mean $\delta^{15}N$

238 values of six pyrosomes and one salp specimen was estimated at $5.31 \pm 0.31‰$ and was used

239 as $\delta^{15}N_{primary\ consumer}$ to estimate the trophic position of all upper trophic level individuals that

240 were collected. At MAD-Ridge, the mean $\delta^{15}N$ values of six salps was $4.22 \pm 1.01‰$ and was

241 used as $\delta^{15}N_{primary\ consumer}$ to estimate the trophic position of all individuals sampled.

242　The second model, TPC, is an additive trophic enrichment model with variable isotopic

243　enrichment, estimated from a meta-analysis study on fish muscle (Caut et al. 2009):

244　TEF = -0.281 $\delta^{15}N_{primary\ consumer}$ + 5.879, where TEF is the trophic enrichment factor

245　TPC = 2.0 + [($\delta^{15}N_i$ - $\delta^{15}N_{primary\ consumer}$)/TEF]　　　　　　　Eq. 2

246　2.5.4 Micronekton habitat ranges and feeding mode

247　Information on habitat ranges of selected micronekton individuals was obtained from the

248　literature (Clarke & Lu, 1975; Pearcy et al., 1977; Smith & Heemstra, 1986; van der Spoel &

249　Bleeker, 1991; Brodeur & Yamamura, 2005; Davison et al., 2015; Romero-Romero et al.,

250　2019). Organisms were classified as being epipelagic (<200 m), mesopelagic (from 200 to

251　1000 m), bathypelagic (below 1000 m to ~100 m from the seafloor) and benthopelagic (living

252　near the bottom) according to definitions of the vertical zonation of the pelagic ocean from

253　Del Giorgio & Duarte (2002) and Sutton (2013). The feeding modes of gelatinous plankton

254　and selected micronekton were obtained from the literature and are summarised in

255　Supplementary Material, Table 2. Organisms were classified into the four trophic groups

256　filter-feeders (salps and pyrosomes), detritivores (leptocephali), omnivores (mainly

257　crustaceans and the fish species *Ceratoscopelus warmingii*) and carnivores (most

258　mesopelagic fish and squid). Crustaceans were classified as omnivores because they prey on

259　zooplankton, such as euphausiids and copepods and are also known for occasional herbivory

260　(Hopkins et al., 1994; Birkley & Gulliksen, 2003; Mauchline, 1959; Foxton & Roe, 1974).

261　Most mesopelagic fish were classified as carnivores because they were reported to be

262　zooplankton feeders, preying on copepods, amphipods, euphausiids and ostracods

263　(Dalpadado & Gjøsæter, 1988; Pakhomov et al., 1996; Tanaka et al., 2007; Hudson et al.,

264　2014; Bernal et al., 2015; Carmo et al., 2015; Young et al., 2015), with no herbivorous

265　feeding strategy except *C. warmingii*, which has developed an adaptive response to

266 competition in low-productive environments (Robison, 1984). For species with unknown

267 diets, the feeding mode was determined based on the feeding habit identified from species

268 within the same genus.

269 In order to give an overview of the foodwebs at the La Pérouse and MAD-Ridge seamounts,

270 hierarchical cluster analyses (average grouping methods) were carried out on resemblance

271 matrices (calculated using Euclidean distances) of normalised $\delta^{13}C$ and $\delta^{15}N$ values per

272 gelatinous plankton and micronekton species at each seamount and for all sampled stations in

273 PRIMER v6 software according to Clarke & Warwick (2001). Further cluster analyses were

274 performed on log-transformed $\delta^{13}C$ values and normalised $\delta^{13}C$ and $\delta^{15}N$ values of

275 micronekton (excluding the outliers salps, pyrosomes, *Funchalia* sp. and leptocephali) for

276 each seamount.

277 2.5.5 Effect of size on $\delta^{15}N$ values of micronekton

278 The size distributions of all gelatinous and micronekton organisms captured during the La

279 Pérouse and MAD-Ridge cruises were heavily right-skewed with most organisms being <100

280 mm in length due to net catchability and selectivity. To test for the effect of size on $\delta^{15}N$

281 values, gelatinous and micronekton organisms <100 mm were considered and linear

282 regressions were computed. Linear models were developed to investigate the effect of body

283 lengths on $\delta^{13}C$ and $\delta^{15}N$ values of gelatinous and micronekton individuals and to investigate

284 the difference in $\delta^{15}N$ values with respect to size between La Pérouse and MAD-Ridge.

285 Additionally, eight micronekton specimens were selected according to their common

286 occurrence at both seamounts, relatively large sample sizes and wide body length ranges, and

287 their $\delta^{15}N$ values were compared between the two seamounts. Information on the migration

288 patterns of these eight taxa was obtained from the literature (Utrecht et al., 1987; Butler et al.,

289 2001; Feunteun et al., 2015; Romero-Romero et al., 2019). Linear regressions were fitted to

290 $\delta^{15}N$ values of these eight taxa according to their body lengths and the seamount factor

291 (whether $\delta^{15}N$ values were significantly different between La Pérouse and MAD-Ridge).To

292 investigate if the seamount has an effect on the size and related diet of fish, $\delta^{15}N$ values of

293 selected omnivorous/ carnivorous fish species collected on the summits, flanks, vicinity of

294 the seamounts and the southern Mozambique Channel, were examined using linear models.

3. Results

3.1 Prevailing environmental conditions at La Pérouse and MAD-Ridge seamounts

297 Sea surface chlorophyll concentrations followed the same seasonal pattern in both regions of

298 La Pérouse and MAD-Ridge seamounts, although concentrations were twice as high at

299 MAD-Ridge (0.10-0.22 mg m^{-3}) than at La Pérouse (0.04-0.13 mg m^{-3}) all year round (Fig.

300 2). A peak in productivity was observed in July in both the ISSG and EAFR provinces

301 because of intense mixing caused by austral trade winds. Both La Pérouse and MAD-Ridge

302 cruises took place during a declining phase of oceanic productivity in the region.

3.2 General foodweb structure

304 The description of the foodweb structure included POM collected at the surface (POM-Surf)

305 and at the depth of maximum fluorescence (POM-Fmax), zooplankton at both seamounts,

306 two taxonomic groups of gelatinous organisms (salps and pyrosomes), and 42 and 49

307 taxonomic groups of micronekton, representing 145 and 180 individuals at La Pérouse and

308 MAD-Ridge respectively. At both La Pérouse and MAD-Ridge, the foodweb components

309 were segregated in their $\delta^{13}C$ (La Pérouse: KW, H=170.5, $p < 0.05$; MAD-Ridge: KW,

310 H=268.1, $p < 0.05$) and $\delta^{15}N$ values (La Pérouse: KW, H=153.1, $p < 0.05$; MAD-Ridge: KW,

311 H=127.4, $p < 0.05$) (Fig. 3). POM-Surf and POM-Fmax did not differ significantly in their

312 $\delta^{13}C$ and $\delta^{15}N$ values at both seamounts ($p > 0.05$). At La Pérouse, gelatinous organisms

313 exhibited higher $\delta^{13}C$ values compared with POM-Surf and POM-Fmax ($p < 0.05$), and they

15

314   exhibited lower $\delta^{13}C$ and $\delta^{15}N$ values than crustaceans, fish and squid at both seamounts (p <

315   0.05). Crustaceans, fish and squid did not differ significantly in their $\delta^{15}N$ values (p > 0.05),

316   but they differed in their $\delta^{13}C$ values at La Pérouse (p < 0.05). Crustaceans did not differ

317   significantly from squid in their $\delta^{13}C$ values (p > 0.05), whereas all other categories differed

318   in their $\delta^{13}C$ values at MAD-Ridge (p < 0.05). Squid did not differ significantly from

319   crustaceans and fish in their $\delta^{15}N$ values (p > 0.05), but ^{15}N was more depleted in crustaceans

320   relative to fish at MAD-Ridge (p < 0.05). At La Pérouse (all depths combined), POM,

321   zooplankton and micronekton covered a large $\delta^{13}C$ range of ~11‰ (-17.2 to -28.0‰), with

322   POM-Fmax and the unidentified caridean crustacean representing the lowest and highest

323   values, respectively. The $\delta^{15}N$ values of all micronekton individuals ranged from 2.5‰ (fish:

324   leptocephali) to 13.3‰ (fish: *Coccorella atrata*). At MAD-Ridge (all depths combined),

325   POM, zooplankton and micronekton also covered a large $\delta^{13}C$ range of ~10‰ (-17.1 to -

326   27.2‰), with POM-Surf and the fish species *Chauliodus sloani* representing the lowest and

327   highest values, respectively. The $\delta^{15}N$ values of sampled micronekton individuals ranged

328   from 2.3‰ (fish: leptocephali) to 13.5‰ (fish: *Argyropelecus aculeatus*).

329   Standard ellipse corrected areas (SEA$_c$) refer to the trophic niche widths of the broad

330   categories at La Pérouse and MAD-Ridge. At La Pérouse, POM-Surf and POM-Fmax

331   showed overlapping standard ellipses with the largest SEA$_c$ (3.2 and 3.8‰^{2}, respectively)

332   among all components of the foodweb (Fig. 3). Gelatinous organisms showed the smallest

333   SEA$_c$ of 0.92‰^{2}. Crustaceans, squid and fish had overlapping standard ellipses with SEA$_c$

334   values of 2.3, 1.2 and 2.9‰^{2}, respectively (Fig. 3). At MAD-Ridge, POM-Surf and POM-

335   Fmax also exhibited overlapping standard ellipses (SEAc= 4.8 and 2.0‰^{2}, respectively), but

336   with greater variability in POM-Surf $\delta^{15}N$ values. Crustaceans, squid and fish had

337   overlapping standard ellipses with SEA$_c$ of 3.0, 3.6 and 3.2‰^{2}, respectively.

16

338   The $\delta^{13}C$ and $\delta^{15}N$ values of the foodweb components POM-Surf, POM-Fmax, zooplankton,

339   gelatinous organisms, crustaceans, squid and fish were significantly different between La

340   Pérouse and MAD-Ridge ($\delta^{13}C$: KW, H=474.4, df=13, $p < 0.05$; $\delta^{15}N$: KW, H=311.3, df=13,

341    $p < 0.05$, Fig. 4). Pairwise comparisons showed $\delta^{13}C$ values of POM-Surf, zooplankton and

342   fish to differ significantly between La Pérouse and MAD-Ridge ($p < 0.05$ each). The median

343    $\delta^{13}C$ and $\delta^{15}N$ values of lower trophic level foodweb components: POM-Surf, POM-Fmax

344   and zooplankton were greater at MAD-Ridge ($\delta^{13}C$: -23.1, -24.1, -20.9‰; $\delta^{15}N$: 6.3, 6.1 and

345   8.9‰, respectively) than at La Pérouse ($\delta^{13}C$: -23.7, -24.1, -22.1‰; $\delta^{15}N$: 5.5, 4.9 and 7.5‰,

346   respectively) (Fig. 4). Gelatinous organisms, crustaceans and fish displayed higher median

347    $\delta^{13}C$ values at La Pérouse (-21.5, -18.4 and -18.7‰, respectively) than at MAD-Ridge (-22.4,

348   -18.6 and -19.1‰, respectively) (Fig. 4). Gelatinous organisms, crustaceans, squid and fish

349   also exhibited higher median $\delta^{15}N$ values at La Pérouse (5.2, 9.8, 10.7 and 10.4‰,

350   respectively) compared to MAD-Ridge (3.7, 8.8, 9.5 and 10.0‰, respectively) (Fig. 4) but

351   differences were not statistically significant ($p > 0.05$ each). The $\delta^{13}C$ values of crustaceans,

352   squid and mesopelagic fish encompassed the same narrow range at La Pérouse and MAD-

353   Ridge (-17.2 to -21.0‰ and -17.1 to -21.1‰, respectively). Gelatinous salps and pyrosomes

354   exhibited $\delta^{13}C$ values of -18.2 to -21.7‰ at La Pérouse and -19.0 to -23.5‰ at MAD-Ridge.

355   3.3 Relationships between $\delta^{13}C$ and $\delta^{15}N$ values

356   Ascending the foodweb, from POM-Surf to mesopelagic fish at La Pérouse and MAD-Ridge

357   seamounts, there was a general increase in $\delta^{13}C$ and $\delta^{15}N$ values (Figs. 3 and 4). There was a

358   significantly positive correlation between $\delta^{13}C$ and $\delta^{15}N$ values of all sampled components of

359   the foodweb at La Pérouse and MAD-Ridge seamount stations ($p < 0.05$), with Spearman

360   correlation coefficients of r= 0.74 and r= 0.51, respectively.

361   3.4 Trophic levels at La Pérouse and MAD-Ridge seamounts

17

362 Albeit small differences in trophic positions between the two methods, they both identified

363 the same organisms at the lowest (leptocephali and gelatinous organisms) and highest

364 (mesopelagic fish excluding leptocephali, and squid) trophic positions. For comparison with

365 other studies published in the region (Ménard et al., 2014; Annasawmy et al., 2018), the

366 additive trophic enrichment model with fixed enrichment factor, TPA, (Eq. 1), is explored in

367 further details.

368 Leptocephali showed estimated TL values (from Eq. 1) of 1.9 and 1.8 at both La Pérouse and

369 MAD-Ridge, respectively (Fig. 5). TL values of crustaceans fell between 2.7 (La Pérouse and

370 MAD-Ridge: *Funchalia* sp.) and 3.7 (La Pérouse: Sergestidae; MAD-Ridge: Oplophoridae).

371 Squid had TL values of 3.6 (*Abraliopsis* sp.) and 4.0 (*Histioteuthis* spp.) at La Pérouse. At

372 MAD-Ridge seamount, smaller-sized nektonic squid (26-111 mm DML) displayed TL values

373 of 3.2 (Enoploteuthidae) and 3.6 (*Abraliopsis* sp.), and larger-sized nektonic squid (365-367

374 mm DML) had TL values of 4.0 (*Histioteuthis* spp.) and 4.8 (*O. bartramii*). TL values of fish

375 (excluding leptocephali) fell between 3.2 (*C. warmingii*) and 4.5 (*C. atrata*) at La Pérouse

376 and between 2.6 (*Decapterus macarellus*) and 4.4 (*Stomias longibarbatus*) at MAD-Ridge

377 (Fig. 5). Overall, the TL values of the micronekton broad categories displayed the same range

378 of TL values at both seamounts.

379 3.5 Effect of feeding mode of gelatinous plankton and micronekton on stable isotope values

380 The trophic groups identified by cluster analyses are in general agreement with the postulated

381 feeding habits of the group members at both La Pérouse and MAD-Ridge seamounts,

382 although significant differences exist when individual species are considered. The cluster

383 analyses based on δ^{13}C and δ^{15}N values identified two main groups, designated I and II, and

384 two subgroups within group I and group II at La Pérouse and MAD-Ridge (Fig. 6). At La

385 Pérouse, Group I included the filter-feeding pyrosomes (IA) and the detritivorous

386 leptocephali (IB) that showed similar $\delta^{13}C$ values (-21.5 $\pm$ 0.2 and -20.4 $\pm$ 0.5‰,

387 respectively) and $\delta^{15}N$ values (5.2 $\pm$ 0.2 and 4.9 $\pm$ 2.1‰, respectively). Group IIa compared a

388 single salp specimen ($\delta^{13}C$: -18.2‰ and $\delta^{15}N$: 5.9‰) and an omnivorous crustacean

389 *Funchalia* sp. with similar $\delta^{13}C$ and $\delta^{15}N$ values (-18.7 $\pm$ 0.6 and 7.5 $\pm$ 0.5‰, respectively).

390 All other crustaceans having an omnivorous feeding mode displayed greater $\delta^{15}N$ values

391 (10.0 $\pm$ 1.1‰) and were thus segregated within subgroup IIB along with carnivorous

392 mesopelagic fish and squid (Fig 6). All values are given in mean $\pm$ S.D.

393 At MAD-Ridge, Group I included filter feeding pyrosomes (IA) and salps, and detritivorous

394 leptocephali (IB) which exhibited the most depleted $\delta^{13}C$ and $\delta^{15}N$ values relative to

395 omnivorous and carnivorous micronekton (Fig. 6). Group II was subdivided into Group IIA

396 included the squid *O. bartramii*, the fish *Promethichthys prometheus* and *S. longibarbatus*, all

397 three having carnivorous feeding modes with similar $\delta^{13}C$ values and the highest $\delta^{15}N$ values

398 for the greatest sizes. The single large squid *Histioteuthis* spp. (DML: 367 mm) showed a

399 high $\delta^{15}N$ value of 10.7‰ and a more depleted $\delta^{13}C$ value of -21.0‰ compared with *O.*

400 *bartramii*, *P. prometheus* and *S. longibarbatus*. This squid was hence segregated from

401 subgroup IIA. All other omnivorous and carnivorous organisms exhibited lower $\delta^{15}N$ values

402 (Fig. 6) and were thus included within subgroup IIB. Cluster analyses run on $\delta^{13}C$ and $\delta^{15}N$

403 values of micronekton and excluding the outliers salps, pyrosomes, *Funchalia* sp. and

404 leptocephali, also segregated individuals according to their feeding mode at MAD-Ridge (p <

405 0.05).

406 3.6 Effect of size of micronekton on $\delta^{15}N$ values

407 The $\delta^{15}N$ values of individuals were significantly influenced by their sizes at both La Pérouse

408 ($F_{1,113}$=6.70, p < 0.05) and MAD-Ridge ($F_{1, 160}$= 23.3, p < 0.05), with increasing $\delta^{15}N$ values

409 as the size of the organisms increased (La Pérouse: $\delta^{15}N_{\text{gelatinous and micronekton} <100 \text{ mm}}$= 8.83 +

410 0.02 x Size; MAD-Ridge: $\delta^{15}N_{\text{gelatinous and micronekton} <100 \text{ mm}}= 7.33 + 0.03$ x Size). Eight

411 micronekton species were further selected according to sample size, their common

412 occurrence at both seamounts, their wide body length ranges, differing feeding modes and

413 vertical migration patterns. The $\delta^{15}N$ values of the selected species *Sigmops elongatus*

414 (carnivore; diel vertical migrator) and *C. warmingii* (omnivore; diel vertical migrator) were

415 significantly influenced by their lengths (Fig. 7a, b, Table 1), with higher $\delta^{15}N$ values at La

416 Pérouse than at MAD-Ridge. The $\delta^{15}N$ values of the fish *A. aculeatus* (carnivore, mid-water

417 migrant) and of the crustacean *Funchalia* sp. (omnivore, diel vertical migrator) were

418 significantly influenced by their lengths but were not significantly different between La

419 Pérouse and MAD-Ridge (Fig. 7c, d, Table 1). The mesopelagic fish *D. suborbitalis* and the

420 squid *Abraliopsis* sp. (both carnivores and diel vertical migrators) exhibited the same range of

421 $\delta^{15}N$ values irrespective of size at La Pérouse and MAD-Ridge (Fig. 7e, f, Table 1). For the

422 same body length, *Abraliopsis* sp. showed higher $\delta^{15}N$ values at La Pérouse relative to MAD-

423 Ridge (Fig. 7f). Models fitted to *C. sloani* (carnivore, diel vertical migrator) and leptocephali

424 (detritivore, migrant or non-migrant depending on species) were not significant (Fig. 7g, h,

425 Table 1). The detritivorous leptocephali had varied $\delta^{15}N$ values irrespective of size and

426 irrespective of the sampling location.

427 The $\delta^{15}N$ values of omnivorous/ carnivorous fish collected in the vicinity of the La Pérouse

428 and MAD-Ridge seamounts and in the southern Mozambique Channel were significantly

429 influenced by individual body size ($F_{3,171} = 10.3$, Adjusted $R^2=13.8$, $p < 0.05$) (Fig. 8a).

430 However, there were no significant influence of body size on the $\delta^{15}N$ values of seamount

431 flank- and summit-associated fish species *D. suborbitalis* (La Pérouse and MAD-Ridge), *B.*

432 *fibulatum*, *D. knappi* and *C. japonicus* ($F_{1,10}= 0.07$, $p > 0.05$) at MAD-Ridge. These seamount

433 flank- and summit-associated fish species (Annasawmy et al., 2019; Cherel et al., 2020)

434 exhibited minimum and maximum $\delta^{15}N$ values of 9.8‰ (*B. fibulatum*) and 11.2‰ (*D.*

435 *suborbitalis*) for individuals ranging in size from 38 mm (*D. suborbitalis*) to 328 mm (*C.*

436 *japonicus*) (Fig. 8b). Despite the differing sizes of these seamount flank- and summit-

437 associated fish species, they exhibited an estimated TL value (TPA model) of ~4 at both La

438 Pérouse and MAD-Ridge pinnacles.

439 3.7 Effect of time of day on δ^{13}C and δ^{15}N values at MAD-Ridge seamount

440 Gelatinous and micronekton organisms sampled at MAD-Ridge exhibited similar δ^{13}C values

441 (-19.6 and -19.4‰ respectively) during day and night (W= 3055.5, p > 0.05). However,

442 individuals collected during daylight showed higher median δ^{15}N values (9.22‰) than those

443 collected at night (8.12‰) (W= 4757.5, p < 0.05).

444 3.8 Seamount effect on δ^{13}C and δ^{15}N values of omnivorous/carnivorous fish

445 The δ^{13}C and δ^{15}N values of omnivorous/carnivorous fish had overlapping ranges at La

446 Pérouse flank and vicinity stations as well as overlapping ranges at MAD-Ridge flank,

447 summit and vicinity and Mozambique Channel stations (Fig. 9). There were no significant

448 differences in δ^{13}C (W= 1619, p > 0.05) of omnivorous/carnivorous fish collected between

449 flank stations and the vicinity of La Pérouse seamount, whereas a significant difference was

450 observed for δ^{15}N values between flank (median: 10.1‰) and vicinity (median: 10.8‰)

451 stations (W= 1876, p < 0.05). There was also no significant difference in δ^{13}C values (KW,

452 H= 1.0, df= 2, p > 0.05) of omnivorous/carnivorous fish collected in the southern

453 Mozambique Channel, the vicinity, flank and summit of MAD-Ridge. However, there was a

454 significant difference in δ^{15}N values (KW, H= 8.5, df= 3, p > 0.05) of

455 omnivorous/carnivorous fish collected from the southern Mozambique Channel (median:

456 10.6‰) and in the vicinity of MAD-Ridge (median: 10.0‰).

457

458 **4. Discussion**

459 To our knowledge, this study is the first to investigate trophic interactions of mesopelagic

460 communities at La Pérouse and MAD-Ridge seamounts using δ^{13}C and δ^{15}N stable isotopes.

461 The foodweb components POM-Surf, POM-Fmax, zooplankton, gelatinous organisms and 42

462 and 49 taxonomic groups of micronekton were identified at La Pérouse and MAD-Ridge,

463 respectively. Despite the low sample sizes for some species, our datasets provide a first

464 overview of the trophic relationships of micronekton at both seamounts.

465 4.1 Sampling bias and constraints

466 The full suite of foodweb components could not be sampled at both seamounts because of

467 trawl gear catchability, selectivity and net avoidance of some species of squid and larger fish.

468 Stable isotopes also have numerous limitations in the extent to which they can be used to

469 elucidate complex foodweb dynamics. Isotopic baselines vary seasonally and spatially

470 (Ménard et al., 2014), and organisms or tissues within a single individual may incorporate the

471 isotopic signal of their diets at varying rates, thereby influencing the stable isotope values of

472 individuals (Martínez Del Rio et al., 2009). The use of pelagic tunicates as isotopic baseline

473 in TL calculations can also be problematic because pelagic tunicates may be members of an

474 alternate microbial foodweb (Pakhomov et al., 2019). There have been concerns in previous

475 studies of the inappropriate use of fixed discrimination factors for trophic position

476 estimations (Caut et al., 2009; Hussey et al., 2014). However, as shown in Olivar et al. (2019)

477 for myctophid species, and in our study for zooplankton and micronekton, the methods for

478 trophic position estimates maintained the essential differences among all species.

479 Furthermore, the δ^{15}N values of gelatinous plankton and micronekton were significantly

480 different between day and night samples at MAD-Ridge. This was probably due to the

481 sampling depth, because night-time samples were collected in the shallow, intermediate and

482 deep layers, whereas daylight samples were collected mostly in the deep layer (apart from

483 two leptocephali collected in the shallow depth category). Previous studies found higher δ^{15}N

22

484   and $\delta^{13}C$ values with depth, which have been linked to the increase of $\delta^{15}N$ in POM with

485   depth (Kolasinski et al., 2012; Fanelli et al., 2013). However, as the IYGPT net had no

486   closing device, the effect of sampling depth on $\delta^{13}C$ and $\delta^{15}N$ values of individuals could not

487   be investigated further.

488   Recent studies have cautioned against the use of a fixed additive nitrogen enrichment factor

489   of ~3.2-3.4‰ that is commonly used to estimate the trophic position of an organism relative

490   to its diet. Caut et al. (2009) showed that the consumer taxonomic group and consumer tissue

491   significantly affect the discrimination factor used in trophic level calculations, and Hussey et

492   al. (2014) stressed that the enrichment between consumers and their primary prey items

493   becomes narrower in the upper parts of a food chain. Bastos et al. (2017) developed a novel

494   method using food-specific trophic discrimination factors to estimate trophic positions of

495   omnivorous fish given that plant-based and animal-based materials in diets are not

496   assimilated in the same manner. Olivar et al. (2019) observed small variations in trophic level

497   calculations of mesopelagic fish when using alternative models to estimate trophic positions.

498   However, those authors also concluded that the important differences among species are

499   retained by all trophic models, similarly to the findings of this study.

500   4.2 Trophic interactions at La Pérouse and MAD-Ridge seamounts

501   Particulate organic matter collected at the surface generally consists of phytoplankton,

502   bacteria, faecal pellets and detritus (Riley, 1971; Saino & Hattori, 1987; Fabiano et al., 1993;

503   Dong et al., 2010; Liénart et al., 2017). The $\delta^{13}C$ values of POM (collected at the surface and

504   at the Fmax depth) were different at the La Pérouse and MAD-Ridge seamounts. $\delta^{13}C$

505   baselines can be affected by various processes such as latitude, nutrient source, depth, ocean

506   mixing and primary productivity (Fry, 2006). Research has found that chlorophyll *a*

507   concentrations explained the variability in POM $\delta^{13}C$ values within the EAFR province but

508   not in the ISSG (Annasawmy et al., 2018). Surface chlorophyll *a* concentrations at MAD-

509   Ridge (within the EAFR province) was greater than at La Pérouse (within the ISSG) all year

510   round (Annasawmy et al., 2019), likely a result of terrestrial input of nutrients from the

511   Madagascar landmass, upwelling events on the shelf to the south of Madagascar

512   (Ramanantsoa et al., 2018), offshore advection of this shelf productivity through cross-shelf

513   transport (Noyon et al., 2018) and vertical mixing in the mesoscale eddy system over MAD-

514   Ridge (De Ruijter et al., 2004; Vianello et al., 2020). High levels of photosynthetic rate

515   (currently occurring at the south Madagascar upwelling and being transported south), would

516   induce higher δ^{13}C POM values at MAD-Ridge compared with the oligotrophic La Pérouse

517   (Fry, 1996; Savoye et al., 2003). Surface POM at MAD-Ridge might have possibly been both

518   of marine and terrestrial origin, yielding higher δ^{13}C values relative to surface POM at La

519   Pérouse, which might have consisted of phytoplankton with no terrestrial POM input.

520   The δ^{13}C-δ^{15}N correlations of all foodweb components were not relatively strong at the La

521   Pérouse and MAD-Ridge seamounts (r = 0.74 and 0.51 respectively) at the times of the

522   cruises. A strong correlation during periods of high productivity would have supported the

523   hypothesis of a unique and isotopically homogeneous pelagic food source (Fanelli et al.,

524   2013; Papiol et al., 2013; Preciado et al., 2017), i.e. a single source of carbon for plankton

525   (Fanelli et al., 2009). The relatively weaker correlation observed in our study suggests a wide

526   array of sources of production sustaining the different assemblages once the main input from

527   surface production has decreased (Fanelli et al., 2011a, b; Papiol et al., 2013), or exploitation

528   of organic matter at different stages of degradation from fresh phytodetritus to highly

529   recycled (Fanelli et al., 2009), or refractory materials such as chitin from copepod

530   exoskeleton becoming abundant in sinking marine snow or inorganic carbonates (Polunin et

531   al., 2001). This would be the case in low productive environments such as the ISSG, where

532   production at La Pérouse would be reduced in September (Annasawmy et al., 2019) and thus

24

533 zooplankton would have to expand their food spectrum, as demonstrated by the larger span of

534 their niche widths over the $\delta^{13}C$ range. Alternatively, the $\delta^{13}C$-$\delta^{15}N$ correlations could reflect

535 temporal variations in the baseline isotope values coupled with varying rates of isotopic

536 incorporation (Fanelli et al., 2009, 2011b, 2013). Higher trophic level organisms such as large

537 crustaceans and fish reportedly do not show seasonal patterns in their isotope values owing to

538 their much slower tissue turnover rates (Polunin et al., 2001). Additional seasonal studies are

539 required to investigate POM and resulting zooplankton $\delta^{13}C$ and $\delta^{15}N$ signatures in July when

540 surface oceanic phytoplankton production is enhanced within the ISSG and EAFR provinces

541 (Annasawmy et al., 2018, 2019).

542 Among the mesopelagic organisms sampled, gelatinous plankton exhibited the lowest trophic

543 level (~2), crustaceans showed an intermediate trophic level (~3), and smaller squid and

544 mesopelagic fish exhibited TL values between 3 and 4, as estimated from the TPA method.

545 Assuming a fixed and additive trophic fractionation of 3.2‰ (for comparison with other

546 SWIO studies), the overall range of $\delta^{15}N$ values implied a two-step (3 trophic levels) and

547 three-step (four trophic levels) pelagic food chain at La Pérouse and MAD-Ridge seamounts,

548 respectively. Unfortunately, no top predators were sampled during these cruises to provide

549 information on higher trophic level organisms. Earlier studies within the EAFR province,

550 showed swordfish *Xiphias gladius* collected off the coast of Madagascar to have a TL of ~4.7

551 ($\delta^{15}N$: 14.0 ± 0.59‰). Specimens collected within the ISSG province had a TL of ~5.2 ($\delta^{15}N$:

552 15.1 ± 0.36‰) (Annasawmy et al., 2018). Several authors described the number of trophic

553 levels averaging between four and six in marine ecosystems, from primary consumers to top

554 predators, and appearing higher in coastal environments, reefs and shelves and lower in

555 oceanic upwelling systems (Arreguín-Sánchez et al., 1993; Browder, 1993; Christensen &

556 Pauly, 1993; Bulman et al,, 2002). Similar to those studies, it seems that both La Pérouse and

557 MAD-Ridge seamounts exhibit trophic levels typical of oceanic systems, although small

25

558   variations may exist in the δ^{13}C and δ^{15}N values of an organism's tissues according to various

559   environmental, behavioural and physiological factors (Ménard et al., 2014; Annasawmy et

560   al., 2018).

561   4.3 Influence of feeding mode and size on δ^{13}C and δ^{15}N values

562   The trophic guilds established at La Pérouse and MAD-Ridge seamounts were segregated in

563   terms of δ^{13}C and δ^{15}N values, from depleted (detritivores and filter-feeders) to enriched

564   (omnivores and carnivores) isotope values, highlighting the fact that these trophic guilds

565   consist of species that exploit distinct classes of resources (Bulman et al., 2002; Papiol et al.,

566   2013; Choy et al., 2016). The large range of δ^{13}C values (~17 to -23‰) when gelatinous

567   organisms are considered together with crustaceans, squid and mesopelagic fish suggests that

568   these organisms exploit different sources of production, thus giving rise to different trophic

569   pathways (Ménard et al., 2014). Gelatinous filter feeders such as salps and pyrosomes ingest

570   a variety of suspended particles (Harbou, 2009; Conley, 2017) and leptocephali include a

571   wide range of species feeding on detrital material (Otake et al., 1993) such as larvacean

572   houses and faecal pellets (Lecomte-Finiger et al., 2004; Feunteun et al., 2015) and hence

573   exhibited depleted δ^{13}C values relative to other micronekton broad categories. Species

574   depleted in ^{13}C reportedly feed near the base of the food chain and are closely associated with

575   plankton relative to fish with higher δ^{13}C values (Polunin et al., 2001).

576   Crustacean taxa were at intermediate trophic levels at both seamounts, below that of strict

577   carnivores and above that of detritivores or filter-feeding organisms. Some species of

578   crustaceans would prey on chaetognaths (Heffernan & Hopkins, 1981), molluscs, olive-green

579   debris containing phytoplankton and protists (Hopkins et al., 1994), and they would share

580   common food sources with mesopelagic fish by foraging on copepods, decapods and

581   euphausiids (Fanelli et al., 2009). Similar to previous studies conducted in the SWIO

582   (Ménard et al., 2014; Annasawmy et al., 2018), crustaceans exhibited overlapping isotopic

583   niches with carnivorous mesopelagic fish and squid at both seamounts. The narrow range of

584    $\delta^{13}C$ values and the greater overlap of isotopic niches between crustaceans and carnivorous

585   squid and mesopelagic fish at both seamounts might suggest some degree of similarity in the

586   diet components with low level of resource partitioning and a high level of competition

587   among these broad categories (Fanelli et al., 2009) or alternatively, different diets but with

588   prey items having similar isotopic compositions.

589   Whereas lower trophic level components, POM-Fmax and zooplankton showed significantly

590   different and higher $\delta^{15}N$ values at MAD-Ridge relative to La Pérouse (most likely because

591   of differing productivity and fast turnover rate of these organisms), higher trophic level

592   components such as crustaceans, squid and fish showed no significant differences in their

593    $\delta^{15}N$ values between the two seamounts. There are several hypotheses for similar isotopic

594   signatures of higher trophic levels when baseline levels differ. First, the sampled organisms

595   might not have had time to incorporate the isotopic composition of their most recent diets,

596   especially if transient productivity bouts had impacted the density or composition of their

597   diet. Whereas some studies reported tissue turnover rates of ~0.1-0.2% per day in deep-sea

598   fish (Hesslein et al., 1993), other studies showed a lack of tissue turnover information in more

599   specific mesopelagic families including Myctophidae and Stomiidae (Choy et al., 2012).

600   Second, the difference in the $\delta^{15}N$ values of POM and zooplankton observed at La Pérouse

601   and MAD-Ridge, although significant, may have been too negligible to be reflected in the

602    $\delta^{15}N$ values of higher trophic levels. Third, the number of squid and crustacean specimens

603   analysed for stable isotopes might not be large enough to reflect the full diversity in the

604   isotopic signatures, and hence the apparent lack of variations in $\delta^{15}N$ values for these

605   individuals between the two seamounts. Finally, as a result of movements, zooplankton

606   grazers and subsequent trophic levels might have fed on prey components that are not those

27

607   sampled in the water column, leading to a mismatch in isotopic signatures between lower and

608   higher trophic levels.

609   In this study, δ^{15}N values of micronekton were correlated to body size. This phenomenon was

610   observed in various organisms such as phytoplankton, zooplankton, decapods and fish and

611   across numerous studies (Sholto-Douglas et al., 1991; France et al., 1998; Waite et al., 2007;

612   Ventura & Catalan, 2008; Hirch & Christiansen, 2010; Choy et al., 2012, 2015; Papiol et al.,

613   2013) and is probably attributable to size-related predation. As organisms grow in size, they

614   can feed farther up the foodweb on larger prey with greater δ^{15}N values (Parry, 2008; Ménard

615   et al., 2014). For those species whose δ^{15}N values (*S. elongatus*, *C. warmingii* and

616   *Abraliopsis* sp.) were significantly influenced by size, their δ^{15}N values were greater (around

617   1‰ difference) at La Pérouse than at MAD-Ridge for the same body lengths. As suggested in

618   Parry (2008), if the δ^{15}N values, and hence the TL of an organism, are influenced by size,

619   then the δ^{15}N signal will also depend on baseline values and the variables that affect an

620   organism's size such as feeding mode, growth rate, body condition and available prey items.

621   As δ^{15}N values of POM and zooplankton were higher at MAD-Ridge than at La Pérouse, we

622   hypothesize that those intermediate TLs at the oligotrophic La Pérouse seamount had a

623   different trophic functioning, with the diet of those species being based on a larger proportion

624   of higher TL prey than at MAD-Ridge.

625   Body size did not have an effect on δ^{15}N values of leptocephali which encompass a wide

626   range of species having a detritivorous and opportunistic feeding mode at both seamounts.

627   Such lack of effect was also observed for *C. sloani* individuals ranging in size from 66 to 184

628   mm at La Pérouse and from 77 to 199 mm at MAD-Ridge. These individuals are semi-

629   migrants, caught in deep and intermediate trawls during both day and night. Individuals 45-

630   178 mm long feed on myctophids and other fish species (Utrecht et al., 1987; Butler et al.,

631   2001) with prey items being more than 63% of their own length (Clarke, 1982). Smaller

632 individuals were reported to feed on euphausiids (Butler et al., 2001). Our trawls failed to

633 capture smaller *C. sloani* individuals which may have had a different diet and possibly

634 different δ^{15}N values relative to larger individuals. There might also be a trophic plateau

635 whereby subsequent increases in trophic position with size are not possible due to physical

636 constraints on the organism or lack of appropriate prey of higher trophic levels, as was

637 observed with *O. bartramii* specimens from the Central North Pacific (Parry, 2008).

638 4.4 Seamount effect on δ^{13}C and δ^{15}N values of fish species

639 Omnivorous/carnivorous fish sampled in the southern Mozambique Channel exhibited

640 slightly enriched δ^{15}N values relative to those sampled in the vicinity of the MAD-Ridge

641 seamount. Productivity in the southern Mozambique Channel may be both entrained from the

642 African landmass and locally generated within mesoscale eddies, hence leading to enhanced

643 chlorophyll *a* concentration, micronekton abundances and enriched δ^{15}N values within tissues

644 of micronekton (Tew-Kai & Marsac, 2009; Annasawmy et al., 2018). For an increase in

645 phytoplankton biomass to take place at the seamounts, physical processes leading to retention

646 (e.g. Taylor columns trapping a body of water), enrichment (e.g. localised upwelling and

647 uplift of nutrients) and concentration of productivity must co-occur (Bakun, 2006). However,

648 as seen at La Pérouse and MAD-Ridge seamounts, the current speeds were too strong during

649 the cruise, and the seamount structures unfavourable for Taylor column formation and for

650 significant retention and assimilation of productivity (Annasawmy et al., 2020). This would

651 have inhibited any subsequent energy transfer to higher trophic levels, potentially explaining

652 the lack of differences in δ^{15}N values between the seamount and the area not influenced by

653 the seamount.

654 Seamount-associated fish species *D. suborbitalis*, *B. fibulatum* and *C. japonicus* (Annasawmy

655 et al., 2019; Cherel et al., 2020), sampled at the summit and on the flanks of MAD-Ridge

656   showed similar δ^{13}C, δ^{15}N and TL values irrespective of their size, similarly to *D.*

657   *suborbitalis* sampled at La Pérouse. This most likely reflects similar food sources at the

658   summit and flanks of both pinnacles or ingestion of different prey items having similar

659   isotopic composition. These fish may associate with the La Pérouse and MAD-Ridge

660   summits and flanks owing to enhanced availability of prey and/or the quiescent shelters

661   offered by the topography (Annasawmy et al., 2019). All seamount-associated fish

662   individuals collected on the summit and flanks of La Pérouse and MAD-Ridge with the

663   IYGPT net were adults, previously reported to prey on copepods (Go, 1986; Olivar et al.,

664   2019; Vipin et al., 2018) and chaetognaths (Appelbaum, 1982), organisms present in similar

665   proportions on and away from both seamounts (Noyon et al., 2020).

666   Although δ^{13}C and δ^{15}N values may depend on a range of factors, there were few differences

667   between δ^{13}C and δ^{15}N values of mesopelagic fish sampled at La Pérouse and MAD-Ridge

668   and those collected in the Indian Ocean, within the oligotrophic ISSG province (*A. aculeatus*

669   δ^{13}C and δ^{15}N values: -18.6 and 9.5‰, *C. sloani*: -18.1 and 9.5‰, and *L. gemellarii*: -18.5

670   and 9.9‰; Annasawmy et al., 2018) and the western Mozambique Channel (*A. aculeatus*: -

671   18.4 and 10.0‰ and *L. gemellarii*: -18.4 and 11.1‰; Annasawmy et al., 2018). Even though

672   mesopelagic fish exhibit small variations in their δ^{13}C and δ^{15}N values across different

673   studies in various oceanic environments, they generally occupy trophic positions between 2

674   and 4, irrespective of the approach used to estimate trophic positions (Fanelli et al., 2011b;

675   Choy et al., 2012, 2015, 2016; Colaço et al., 2013; Ménard et al., 2014; Valls et al., 2014a,b;

676   Denda et al., 2017; Annasawmy et al., 2018; Olivar et al., 2019). Despite the possible bias

677   induced by the different time-scales in sampling (Mill et al., 2008), within a stable isotope

678   approach, the trophic positions of mesopelagic fish across numerous studies confirmed

679   similar dietary patterns and food sources with similar isotopic compositions. Hence, these

680　mesopelagic fish species by their opportunistic feeding mode may play a similar trophic role

681　across different environments (Olivar et al., 2019).

682　**Concluding Remarks**

683　This study has shown that despite the different productivity at the two shallow seamounts and

684　the significant differences in lower trophic level δ^{13}C and δ^{15}N values, crustaceans, smaller-

685　sized squid and mesopelagic fish, because of their varied feeding modes, occupy trophic

686　positions between 3 and 4. Specimen size had an influence on the δ^{15}N values of most

687　individuals, although that also depended on the life strategy and feeding mode of the species

688　considered. The δ^{13}C and δ^{15}N values of mesopelagic organisms sampled during both cruises

689　reflected those of typical oceanic systems and the seamounts did not seem to have any impact

690　on the overall isotopic signatures of the mesopelagic taxa sampled. However, the few

691　seamount-associated/resident fish sampled showed similar δ^{15}N values and trophic levels

692　irrespective of their size at the summits and flanks of the pinnacles. La Pérouse and MAD-

693　Ridge seamounts may hence be important foraging grounds for the few taxa that

694　preferentially associate with their slopes and summits, and thus benefit from the varied

695　habitat types that the seamounts offer compared to the open ocean environment.

696

References

Annasawmy, P., Ternon, J.F., Marsac, F., Cherel, Y., Béhagle, N., Roudaut, G., Lebourges-Dhaussy, A., Demarcq, H., Moloney, C.L., Jaquemet, S., Ménard, F., 2018. Micronekton diel migration, community composition and trophic position within two biogeochemical provinces of the South West Indian Ocean: Insight from acoustics and stable isotopes. Deep Sea Research Part I: Oceanographic Research Papers. 138, 85–97. https://doi.org/10.1016/j.dsr.2018.07.002

Annasawmy, P., Ternon, J-F., Cotel, P., Demarcq, H., Cherel, Y, Romanov, E., Roudaut, G., Lebourges-Dhaussy, A., Ménard, F., Marsac, F. 2019. Micronekton distribution and assemblages at two shallow seamounts in the south-western Indian Ocean: Insights from acoustics and mesopelagic trawl data. Progress in Oceanography-accepted.

Annasawmy, P., Ternon, J-F., Lebourges-Dhaussy, A., Roudaut, G., Herbette, S., Ménard, F., Cotel., P., Marsac, F., 2020. Micronekton distribution as influenced by mesoscale eddies, Madagascar shelf and shallow seamounts in the south-western Indian Ocean: An acoustic approach. Deep-Sea Res. II, this issue.

Appelbaum, S., 1982. Studies on food organisms of pelagic fishes as revealed by the 1979 North Atlantic Eel Expedition. Helgoländer Meeresuntersuchungen. 35, 357–367. https://doi.org/10.1007/BF02006143

Arreguín-Sánchez, F., Valero-Pacheco, E., Chávez, E.A., 1993. A Trophic Box Model of the Coastal Fish Communities of the Southwestern Gulf of Mexico. In V. Christensen and D. Pauly (Eds) Trophic Models of Aquatic Ecosystems. ICLARM Conference Proceedings, 26: 390.

Bakun, A., 2006. Fronts and eddies as key structures in the habitat of marine fish larvae: opportunity, adaptive response and competitive advantage. Sci. Mar. 70, 105–122. https://doi.org/10.3989/scimar.2006.70s2105

Bastos, R.F., Corrêa, F., Winemiller, K.O., Garcia, A.M., 2017. Are you what you eat? Effects of trophic discrimination factors on estimates of food assimilation and trophic position with a new estimation method. Ecological Indicators. 75: 234-241. http://dx.doi.org/10.1016/j.ecolind.2016.12.007

Bernal, A., Olivar, M.P., Maynou, F., Fernández de Puelles, M.L., 2015. Diet and feeding strategies of mesopelagic fishes in the western Mediterranean. Progr. Oceanogr. 135, 1-17. https://doi.org/10.1016/j.pocean.2015.03.005

Bertrand, A., Bard, F.X. Josse, E., 2002. Tuna food habits related to the micronekton distribution in French Polynesia. Mar Biol. 140: 1023-1037. DOI: 10.1007/s00227-001-0776-3

Bianchi, D., Stock, C., Galbraith, E.D., Sarmiento, J.L., 2013. Diel vertical migration: Ecological controls and impacts on the biological pump in a one-dimensional ocean model. Global Biogeochem. Cycles. 27: 478-491. DOI: 10.1002/gbc.20031

Birkley, S.-R., Gulliksen, B., Feeding Ecology in Five Shrimp Species (Decapoda, Caridea) from an Arctic Fjord (Isfjorden, Svalbard), with Emphasis on *Sclerocrangon boreas* (Phipps, 1774).

Bodin, N., Budzinski, H., Le Ménach, K., Tapie, N., 2009. ASE extraction method for simultaneous carbon and nitrogen stable isotope analysis in soft tissues of aquatic organisms. Analytica Chimica Acta. 643: 54-60. DOI: 10.1016/j.aca.2009.03.048

Brodeur, R., Yamamura, O., 2005. PICES Scientific Report No. 30 Micronekton of the North Pacific. PICES Scientific Report, Sidney B.C., Canada, pp. 1-115.

Browder, J.A., 1993. A pilot model of the Gulf of Mexico continental shelf. In V. Christensen and D. Pauly (Eds) Trophic Models of Aquatic Ecosystems. ICLARM Conference Proceedings. 26: 390.

Bulman, C.M., He, X., Koslow, J.A., 2002. Trophic ecology of the mid-slope demersal fish community off southern Tasmania, Australia. Mar. Freshwater Res. 53: 59-72. DOI: 10.1071/MF01057

Butler, M., Bollens, S.M., Burkhalter, B., Madin, L.P., Horgan, E., 2001. Mesopelagic fishes of the Arabian Sea: distribution, abundance and diet of *Chauliodus pammelas*, *Chauliodus sloani*, *Stomias aznis*, and *Stomias nebulosus*. Deep-Sea Res. II. 48: 1369-1383.

Carmo, V., Sutton, T., Menezes, G., Falkenhaug, T., Bergstad, O.A., 2015. Feeding ecology of the Stomiiformes (Pisces) of the northern Mid-Atlantic Ridge. 1. The Sternoptychidae and Phosichthyidae. Prog. Oceanogr. 130: 172-187. https://doi.org/10.1016/j.pocean.2014.11.003

Catul, V., Gauns, M., Karuppasamy, P.K., 2011. A review of mesopelagic fishes belonging to family Mcytophidae. Rev. Fish Biol. Fisheries. 21: 339-354. DOI: 10.1007/s11160-010-9176-4

Caut, S., Angulo, E., Courchamp, F., 2009. Variation in discrimination factors (Δ^{15}N and Δ^{13}C): the effect of diet isotopic values and applications for diet reconstruction. Journal of Applied Ecology. 46: 443-453. DOI: 10.1111/j.1365-2664.2009.01620.x

Cherel, Y., Fontaine, C., Richard, P., Labat, J.-P., 2010. Isotopic niches and trophic levels of myctophid fishes and their predators in the Southern Ocean. Limnol. Oceanogr. 55, 324–332. https://doi.org/10.4319/lo.2010.55.1.0324

Cherel, Y., Romanov, E.V., Annasawmy, P., Thibault, D., Ménard, F., 2020. Micronektonic fish species over three seamounts in the southwestern Indian Ocean. Deep-Sea Res. II. https://doi.org/10.1016/j.dsr2.2020.104777

Choy, C.A., Davison, P.C., Drazen, J.C., Flynn, A., Gier, E.J., Hoffman, J.C., McClain-Counts, J.P., Miller, T.W., Popp, B.N., Ross, S.W., Sutton, T.T., 2012. Global trophic position comparison of two dominant mesopelagic fish families (Myctophidae, Stomiidae) using amino acid nitrogen isotopic analyses. PLoS One. 7(11): e50133. DOI: 10.1371/journal.pone.0050133

Choy, C.A., Popp, B.N., Hannides, C.C.S., Drazen, J.C., 2015. Trophic structure and food resources of epipelagic and mesopelagic fishes in the North Pacific Subtropical Gyre ecosystem inferred from nitrogen isotopic compositions. Limnol. Oceanogr. 60: 1156-1171.

Choy, C.A., Wabnitz, C.C.C., Weijerman, M., Woodworth-Jefcoats, P.A., Polovina, J.J., 2016. Finding the way to the top: how the composition of oceanic mid-trophic micronekton groups determines apex predator biomass in the central North Pacific. Mar. Ecol. Prog. Ser. 549: 9-25. DOI: 10.3354/meps11680

Christensen, V., Pauly, D., 1993. Flow Characteristics of Aquatic Ecosystems. In V. Christensen and D. Pauly (Eds) Trophic Models of Aquatic Ecosystems. ICLARM Conference Proceedings. 26: 390.

Clarke, M.R., Lu, C.C., 1975. Vertical distribution of cephalopods at 18°N 25°W in the North Atlantic. J. mar. biol. Ass. 55: 165-182. https://doi.org/10.1017/S0025315400015812

Clarke, T.A., 1982. Feeding habits of stomiatoid fishes from Hawaiian waters. Fishery Bulletin. 80(2): 287-304.

Clarke, K., Warwick, R., 2001. Change in Marine Communities: An Approach to Statistical Analysis and Interpretation. PRIMER-E Ltd: Plymouth, United Kingdom.

Clark, M.R., Vinnichenko, V.I., Gordon, J D M , Beck-Bulat, G..Z., Kukharev, N. N., and. Kakora, A.F., 2007. Large-scale distant-water trawl fisheries on seamounts. In:

Pitcher, T. J., Morato, T., Hart, P. J. B., Clark, M. R., Haggan, N., & Santos, R. S. (Eds.). Seamounts: Ecology, Fisheries & Conservation. Blackwell Publishing. 361-399.

Colaço, A., Giacomello, E., Porteiro, F., Menezes, G.M., 2013. Trophodynamic studies on the Condor seamount (Azores, Portugal, North Atlantic). Deep-Sea Res. Part II: Topical Studies in Oceanography. 98: 178–189. https://doi.org/10.1016/j.dsr2.2013.01.010

Conley, K.P., 2017. Mechanics and Selectivity of filtration by tunicates. PhD thesis, University of Oregon, USA.

Cresson, P., Ruitton, S., Fontaine, M-F., Harmelin-Vivien, M., 2012. Marine Pollution Bulletin. 1112-1121. http://dx.doi.org/10.1016/j.marpolbul.2012.04.003

Dalpadado, P., Gjøsæter, J., 1988. Feeding ecology of the lanternfish *Benthosema pterotum* from the Indian Ocean. Mar. Biol. 99: 555-567.

Daly, R., Froneman, P.W., Smale, M.J., 2013. Comparative Feeding Ecology of Bull Sharks (*Carcharhinus leucas*) in the Coastal Waters of the Southwest Indian Ocean Inferred from Stable Isotope Analysis. PLoS ONE 8(10): e78229. doi:10.1371/journal.pone.0078229

Danckwerts, D.K., McQuaid, C.D., McGregor, G.K., Dwight, R., Le Corre, M., Jaquemet, S., 2014. Biomass consumption by breeding seabirds in the western Indian Ocean: indirect interactions with fisheries and implications for management. ICES Journal of Marine Science. 71(9): 2589-2598. DOI: 10.1093/icesjms/fsu093

Davison, P. C., Koslow, J. A., Kloser, R. J., 2015. Acoustic biomass estimation of mesopelagic fish: backscattering from individuals, populations, and communities. ICES Jour. Mar. Sci. 72(5), 1413-1424. https://doi.org/10.1093/icesjms/fsv023

De Forest, L., Drazen, J., 2009. The influence of a Hawaiian seamount on mesopelagic micronekton. Deep-Sea Res. I. 56: 232-250. DOI: 10.1016/j.dsr.2008.09.007

Del Giorgio, P.A., Duarte, C.M., 2002. Respiration in the open ocean. Nature. 420: 379-384.

Denda, A., Stefanowitsch, B., Christiansen, B., 2017. From the epipelagic zone to the abyss: Trophic structure at two seamounts in the subtropical and tropical Eastern Atlantic- Part I zooplankton and micronekton. Deep Sea Res. Part I. 130: 63-77.

De Ruijter, W.P.M., Aken, H.M. van, Beier, E.J., Lutjeharms, J.R.E., Matano, R.P., Schouten, M.W., 2004. Eddies and dipoles around South Madagascar: formation, pathways and large-scale impact. Deep Sea Res. Part Oceanogr. Res. Pap. 51: 383–400. https://doi.org/10.1016/j.dsr.2003.10.011

Dong, H-P., Wang, D-Z., Dai, M., Hong, H-S., 2010. Characterization of particulate organic matters in the water column of the South China Sea using a shotgun proteomic approach. Limnol. Oceanogr. 55(4): 1565-1578. DOI: 10.4319/lo.2010.55.4.1565

Dower, J., Freeland, H., Juniper, K., 1992. A strong biological response to oceanic flow past Cobb Seamount. Deep Sea Res. Part Oceanogr. Res. Pap. 39: 1139–1145. https://doi.org/10.1016/0198-0149(92)90061-W

Dubroca, L., Chassot, E., Floch, L., Demarcq, H., Assan, C., Delgado de Molina, A., 2013. Seamounts and tuna fisheries: Tuna hotspots or fishermen habits? Collect. Vol. Sci. Pap. ICCAT. 69(5): 2087-2102.

Duffy, L.M., Kuhnert, P.M., Pethybridge, H.R., Young, J.W., Olson, R.J., Logan, J.M., Goñi, N., Romanov, E., Allain, V., Staudinger, M.D., Abecassis, M., Choy, C.A., Hobday, A.J., Simier, M., Galván-Magaña, F., Potier, M., Ménard, F., 2017. Global trophic ecology of yellowfin, bigeye, and albacore tunas: Understanding predation on micronekton communities at ocean-basin scales. Deep-Sea Res. II. 40: 55-73.

http://dx.doi.org/10.1016/j.dsr2.2017.03.003

Fabiano, M., Povero, P., Danovaro, R., 1993. Distribution and composition of particulate organic matter in the Ross Sea (Antarctica). Polar Biol. 13: 525-533.

Fanelli, E., Cartes, J.E., Rumolo, P., Sprovieri, M., 2009. Food-web structure and trophodynamics of mesopelagic-suprabenthic bathyal macrofauna of the Algerian Basin based on stable isotopes of carbon and nitrogen. Deep-Sea Res. I. 56: 1504-1520.
DOI: 10.1016/j.dsr.2009.04.004

Fanelli, E., Papiol, V., Cartes, J.E., Rumolo, P., Brunet, C., Sprovieri, M., 2011a. Food web structure of the epibenthic and infaunal invertebrates on the Catalan slope (NW Mediterranean): Evidence from $\delta^{13}C$ and $\delta^{15}N$ analysis. Deep-Sea Res. I: Oceanographic Research Papers. 58: 98–109.
https://doi.org/10.1016/j.dsr.2010.12.005

Fanelli, E., Cartes, J.E., Papiol, V., 2011b. Food web structure of deep-sea macrozooplankton and micronekton off the Catalan slope: Insight from stable isotopes. Journal of Marine Systems. 87: 79-89. DOI: 10.1016/j.jmarsys.2011.03.003

Fanelli, E., Papiol, V., Cartes, J.E., Rumolo, P., López-Pérez, C., 2013. Trophic webs of deep-sea megafauna on mainland and insular slopes of the NW Mediterranean: a comparison by stable isotope analysis. Mar. Ecol. Prog. Ser. 490: 199-221.
DOI: 10.3354/meps10430

Feunteun, E., Miller, M.J., Carpentier, A., Aoyama, J., Dupuy, C., Kuroki, M., Pagano, M., Réveillac, E., Sellos, D., Watanabe, S., Tsukamoto, K., Otake, T., 2015. Stable isotopic composition of anguiliform leptocephali and other food web components from west of the Mascarene Plateau. Prog. Oceanogr. 137: 69-83.
http://dx.doi.org/10.1016/j.pocean.2015.05.024

Fonteneau, A., 1991. Monts sous-marins et thons dans l'Atlantique tropical est. Aquat. Living. Resour. 4: 13-25.

Foxton, P., Roe, H.S.J., 1974. Observations on the Nocturnal Feeding of some Mesopelagic Decapod Crustacea. Mar. Biol. 28: 37-49.

France, R., Chandler, M., Peters, R., 1998. Mapping trophic continua of benthic foodwebs: body size-δ15N relationships. Mar. Ecol. Prog. Ser. 174: 301-306.

Fry, B., 1996. $^{13}C/^{12}C$ fractionation by marine diatoms. Mar. Ecol. Prog. Ser. 134: 283-294.

Fry, B., 2006. Stable Isotope Ecology. Springer, New York. 308pp.

Genin, A., Boehlert, G.W., 1985. Dynamics of temperature and chlorophyll structures above a seamount: An oceanic experiment. J. Mar. Res. 43: 907–924.
https://doi.org/10.1357/002224085788453868

Go, Y.B., 1986. Diet and feeding chronology of mesopelagic micronektonic fish, *Diaphus suorbitalis*, in Suruga Bay, Japan. In: 1. Asian Fisheries Forum, Manila (Philippines), 26-31 May 1986.

Guinet, C., Cherel, Y., Ridoux, V., Jouventin, P., 1996. Consumption of marine resources by seabirds and seals in Crozet and Kerguelen waters: changes in relation to consumer biomass 1962-85. Antarctic Science. 8(1): 23-30

Halo, I., Backeberg, B., Penven, P., Ansorge, I., Reason, C., Ullgren, J.E., 2014. Eddy properties in the Mozambique Channel: A comparison between observations and two numerical ocean circulation models. Deep Sea Res. Part II Top. Stud. Oceanogr. 100: 38-53. http://dx.doi.org/10.1016/j.dsr2.2013.10.015

Harbou, L.V., 2009. Trophodynamics of salps in the Atlantic Southern Ocean. PhD thesis, Universität Bremen, Germany.

Heffernan, J.T., Hopkins, T.L., 1981. Vertical Distribution and Feeding of the Shrimp Genera *Gennadas* and *Bentheogennema* (Decapoda: Penaeida) in the Eastern Gulf of Mexico. Journal of Crustacean Biology. 1(4): 461-473.

Hesslein, R.H., Hallard, K.A., Ramlal, P., 1993. Replacement of Sulfur, Carbon, and Nitrogen in Tissue of Growing Broad Whitefish (Coregonus nasus) in Response to a Change in Diet Traced by δ34S, δ13C, and δ15N. Can. J. Fish. Aquat. Sci. 50: 2071-2076.

Hidaka, K., Kawaguchi, K., Murakami, M., Takahashi, M., 2001. Downward transport of organic carbon by diel migratory micronekton in the western equatorial Pacific: its quantitative and qualitative importance. Deep-Sea Res. I. 48: 1923-1939

Hirch, S., Christiansen, B., 2010. The trophic blockage hypothesis is not supported by the diets of fishes on Seine Seamount. Marine Ecology. 31: 107–120. https://doi.org/10.1111/j.1439-0485.2010.00366.x

Hobson, K.A., Piatt, J.F., Pitocchelli, J., 1994. Using stable isotopes to determine seabird trophic relationships. Journal of Animal Ecology. 63: 786-798.

Holland, K.N., Kleiber, P., Kajiura, S.M., 1999. Different residence times of yellowfin tuna, *Thunnus albacares*, and bigeye tuna, *T. obesus*, found in mixed aggregations over a seamount. Fish. Bull. 97: 392–395.

Hopkins, T.L., Flock, M.E., Gartner, J.V. Jr., Torres, J.J., 1994. Structure and trophic ecology of a low latitude midwater decapod and mysid assemblage. Mar. Ecol. Prog. Ser. 109: 143-156.

Hudson, J.M., Steinberg, D.K., Sutton, T.T., Graves, J.E., Latour, R.J., 2014. Myctophid feeding ecology and carbon transport along the northern Mid-Atlantic Ridge. Deep-Sea Res. I. 93:104-116. https://doi.org/10.1016/j.dsr.2014.07.002

Hussey, N.E., MacNeil, M.A., McMeans, B.C., Olin, J.A., Dudley, S.F.J., Cliff, G., Wintner, S.P., Fennessy, S.T., Fisk, A.T., 2014. Rescaling the trophic structure of marine food webs. Ecology Letters, 17: 239-250. DOI: 10.1111/ele.12226

Ingole, B., Koslow, J.A., 2005. Deep-sea ecosystems of the Indian Ocean. Indian Journal of Marine Sciences. 34(1): 27-34.

IOTC Catch and Effort database. 2018. Available at https://www.iotc.org/data/datasets?__cf_chl_jschl_tk__=ebffbdbd808fe0fa2e0ce342d88a0e0fa97fc63c-1578403316-0-AbYRwW88C8MO-1LnSVqSvpMqY3x_PGoxouNKuvgZy2X8De9NCy6mFx07f7GFtJjokedKCvEkJ5b7BwcYQtIX-A4KidGt1a6J9aAY9H8Y2ormKM543ixwdYh8d0HrniHi9P31fM1U8qyHBGexlhPFKYzXUxMKbV509-vD1mrSjYwW77ozbytXjlWcy3O2h_1C12C2-RJGWCsaxE2gxxw4xIWzXEFZ4tCh-YqOZRzXUpqxNgWBVaOxSTgNMboZj9PAKa1dIsFRs93SwtgNflbIgQg

Jackson, A.L., Inger, R., Parnell, A.C., Bearhop, S., 2011. Comparing isotopic niche widths among and within communities: SIBER – Stable Isotope Bayesian Ellipses in R. Journal of Animal Ecology. 80: 595-602. DOI: 10.1111/j.1365-2656.2011.01806.x

Jaquemet, S., Ternon, J.F., Kaehler, S., Thiebot, J.B., Dyer, B., Bemanaja, E., Marteau, C., Le Corre, M., 2014. Contrasted structuring effects of mesoscale features on the seabird community in the Mozambique Channel. Deep-Sea Res. II. 100: 200-211. http://dx.doi.org/10.1016/j.dsr2.2013.10.027

Kolasinski, J., Rogers, K., Frouin, P., 2008. Effects of acidification on carbon and nitrogen stable isotopes of benthic macrofauna from a tropical coral reef. Rapid Commun Mass Spectrom. 22: 2955–2960. DOI: 10.1002/rcm.3694

Kolasinski, J., Kaehler, S., Jaquemet, S., 2012. Distribution and sources of particulate organic matter in a mesoscale eddy dipole in the Mozambique Channel (south-western Indian

Ocean): Insight from C and N stable isotopes. J. Mar. Syst. 96-97: 122-131. https://doi.org/10.1016/j.jmarsys.2012.02.015

Karakulak, F.S., Salman, A., Oray, I.K., 2009. Diet composition of bluefin tuna (*Thunnus thynnus* L. 1758) in the Eastern Mediterranean Sea, Turkey. J. Appl. Ichthyol. 25: 757-761. DOI: 10.1111/j.1439-0426.2009.01298.x

Koslow, J.A., 1997. Seamounts and the Ecology of Deep-Sea Fisheries: The firm-bodied fishes that feed around seamounts are biologically distinct from their deepwater neighbors-and may be especially vulnerable to overfishing. American Scientist. 85(2): 168-176.

Lack, M., Short, K., Willock, A., 2003. Managing risk and uncertainty in deep-sea fisheries: lessons from Orange Roughy. TRAFFIC Oceania and WWF Endangered Seas Programme.

Layman, C.A., Arrington, D.A., Montaña, C.G., Post, D.M., 2007. Can stable isotope ratios provide for community-wide measures of trophic structure? Ecology. 88: 42–48.

Lecomte-Finiger, R., Maunier, C., Khafif, M., 2004. Leptocephali, these unappreciated larvae. Cybium. 28(2): 83-95.

Liénart, C., Savoye, N., Bozec, Y., Breton, E., Conan, P., David, V., Feunteun, E., Grangeré, K., Kerhervé, P., Lebreton, B., Lefebvre, S., L'Helguen, S., Mousseau, L., Raimbault, P., Richard, P., Riera, P., Sauriau, P.-G., Schaal, G., Aubert, F., Aubin, S., Bichon, S., Boinet, C., Bourasseau, L., Bréret, M., Caparros, J., Cariou, T., Charlier, K., Claquin, P., Cornille, V., Corre, A.-M., Costes, L., Crispi, O., Crouvoisier, M., Czamanski, M., Del Amo, Y., Derriennic, H., Dindinaud, F., Durozier, M., Hanquiez, V., Nowaczyk, A., Devesa, J., Ferreira, S., Fornier, M., Garcia, F., Garcia, N., Geslin, S., Grossteffan, E., Gueux, A., Guillaudeau, J., Guillou, G., Joly, O., Lachaussée, N., Lafont, M., Lamoureux, J., Lecuyer, E., Lehodey, J.-P., Lemeille, D., Leroux, C., Macé, E., Maria, E., Pineau, P., Petit, F., Pujo-Pay, M., Rimelin-Maury, P., Sultan, E., 2017. Dynamics of particulate organic matter composition in coastal systems: A spatio-temporal study at multi-systems scale. Progress in Oceanography 156: 221–239. https://doi.org/10.1016/j.pocean.2017.03.001

Longhurst, A., 1998. Ecological Geography of the Sea. Academic Press, San Diego. 398p.

Longhurst, A., 2007. The Indian Ocean-Indian South Subtropical Gyre Province (ISSG). In: Academic Press (Ed.), Ecological Geography of the Sea, 2nd ed. Elsevier, USA, pp 285.

Lorrain, A., Graham, B.S., Popp, B.N., Allain, V., Olson, R.J., Hunt, B.P.V., Potier, M., Fry, B., Galván-Magaña, F., Menkes, C.E.R., Kaehler, S., Ménard, F., 2015. Nitrogen isotopic baselines and implications for estimating foraging habitat and trophic position of yellowfin tuna in the Indian and Pacific Oceans. Deep-Sea Res. II. 113: 188-198.
https://doi.org/10.1016/j.dsr2.2014.02.003

Marsac, F., Fonteneau, A., Michaud, P., 2014. Le « Coco de Mer », une montagne sous la mer. In: L'or bleu des Seychelles: Histoire de la pêche industrielle au thon dans l'océan Indien. IRD Editions. 151-163.

Marsac, F., Annasawmy, P., Noyon, M., Demarcq, H., Soria, M., Rabearisoa, N., Bach, P., Cherel, Y., Grelet, J., Romanov, E., 2020. Seamount effect on circulation and distribution of ocean taxa at and near La Pérouse, a shallow seamount in the southwestern Indian Ocean. Deep-Sea II.

Martínez del Rio, C., Wolf, N., Carleton, S.A., Gannes, L.Z., 2009. Isotopic ecology ten years after a call for more laboratory experiments. Biol. Rev. 84: 91-111.
DOI: 10.1111/j.1469-185X.2008.00064.x

Mauchline, J., The Biology of the Euphausiid Crustacean, *Meganyctiphanes norvegica* (M. Sars). Proceedings of the Royal Society of Edinburgh, Section B: Biological Sciences. 67(2): 141-179

Ménard, F., Benivary, H.D., Bodin, N., Coffineau, N., Le Loc'h, F., Mison, T., Richard, P., Potier, M., 2014. Stable isotope patterns in micronekton from the Mozambique Channel. Deep-Sea Research Part II: Topical Studies in Oceanography 100, 153–163. https://doi.org/10.1016/j.dsr2.2013.10.023

Michener, R.H., Kaufman, L., 2007. Stable isotope ratios as tracers in marine food webs: an update. R.H. Michener, K. Lajtha (Eds.), Stable Isotopes in Ecology and Environmental Science (2nd ed.), Blackwell, Malden, MA (2007). pp. 238-282.

Mill, A.C., Sweeting, C.J., Barnes, C., Al-Habsi, S.H., MacNeil, M.A., 2008. Mass-spectrometer bias in stable isotope ecology. Limnol. Oceanogr: Methods. 6(1): 34-39.

Minagawa, M., Wada, E., 1984. Stepwise enrichment of ^{15}N along food chains: further evidence and the relation between δ^{15}N and animal age. Geochim. Cosmochim. Acta. 48: 1135-1140.

Mohn, C., White, M., 2007. Remote sensing and modelling of bio-physical distribution patterns at Porcupine and Rockall Bank, Northeast Atlantic. Cont. Shelf Res. 27: 1875-1892. DOI:10.1016/j.csr.2007.03.006

Morato, T., Varkey, D.A., Damaso, C., Machete, M., Santos, M., Prieto, R., Santos, R.S., Pitcher, T.J., 2008. Evidence of a seamount effect on aggregating visitors. Mar. Ecol. Prog. Ser. 357: 23-32. DOI: 10.3354/meps07269

Morato, T., Hoyle, S.D., Allain, V., Nicol, S.J., 2010. Tuna longline fishing around West and Central Pacific seamounts. PLoS ONE. 5(12): e14453.
DOI: 10.1371/journal.pone.0014453

Mouriño, B., Fernández, E., Serret, P., Harbour, D., Sinha, B., Pingree, R., 2001. Variability and seasonality of physical and biological fields at the Great Meteor Tablemount (subtropical NE Atlantic). Oceanol. Acta 24: 167–185. https://doi.org/10.1016/S0399-1784(00)01138-5

Musyl, M.K., Brill, R.W., Boggs, C.H., Curran, D.S., Kazama, T.K., Seki, M.P., 2003. Vertical movements of bigeye tuna (*Thunnus obesus*) associated with islands, buoys, and seamounts near the main Hawaiian Islands from archival tagging data. Fish. Oceanogr. 12: 152–169. https://doi.org/10.1046/j.1365-2419.2003.00229.x

Noyon, M., Morris, T., Walker, D., Huggett, J., 2018. Plankton distribution within a young cyclonic eddy off south-western Madagascar. Deep Sea Res. Part II Top. Stud. Oceanogr. In Press. https://doi.org/10.1016/j.dsr2.2018.11.001

Noyon, M., Rasoloarijao, Z.T., Huggett, J., Roberts, M., Ternon, J-F., 2020. Comparison of mesozooplankton communities at three shallow seamounts in the South Western Indian Ocean using size spectrum analysis. Deep-Sea Res. II.

Olivar, M.P., Bode, A., López-Pérez, C., Hulley, P.A., Hernández-León, S., 2019. Trophic position of lanternfishes (Pisces: Myctophidae) of the tropical and equatorial Atlantic estimated using stable isotopes. ICES Journal of Marine Science. DOI: 10.1093/icesjms/fsx243.

Otake, T., Nogami, K., Maruyama, K., 1993. Dissolved and particulate organic matter as possible food sources for eel leptocephali. Mar. Ecol. Prog. Ser. 92: 27-34.

Pakhomov, E. A., Perissinotto, R., & McQuaid, C. D., 1996. Prey composition and daily rations of myctophid fishes in the Southern Ocean. Mar. Ecol. Prog. Ser. 134, 1-14.

Pakhomov, E.A., Henschke, N., Hunt, B.P.V., Stowasser, G., Cherel, Y., 2019. Utility of salps as a baseline proxy for food web studies. J. Plankton Res. 1-9.

DOI: 10.1093/plankt/fby051

Papiol, V., Cartes, J.E., Fanelli, E., Rumolo, P., 2013. Food web structure and seasonality of slope megafauna in the NW Mediterranean elucidated by stable isotopes: Relationship with available food sources. Journal of Sea Research, 77: 53-69. http://dx.doi.org/10.1016/j.seares.2012.10.002

Parry, M., 2008. Trophic variation with length in two ommastrephid squids, *Ommastrephes bartramii* and *Sthenoteuthis oualaniensis*. Mar. Biol. 153: 249-256. DOI: 10.1007/s00227-007-0800-3

Paya, I., Montecinos, M., Ojeda, V., Cid, L., 2006. An overview of the orange roughy (*Hoplostethus* sp.) fishery off Chile. In: Shotton, R. (Ed.) Deep Sea 2003: Conference on the Governance and Management of Deep-sea fisheries. Part 2: Conference poster papers and workshop papers. Queenstown, New Zealand, 1-5 December 2003 and Dunedin, New Zealand 27-29 November 2003. FAO Fisheries Proceedings No. 3/2, Rome, FAO. 487 pp.

Pearcy, W.G., Krygier, E.E., Mesecar, R., Ramsey, F., 1977. Vertical distribution and migration of oceanic micronekton off Oregon. Deep-Sea Res. 24: 223-245.

Polunin, N.V.C., Morales-Nin, B., Pawsey, W.E., Cartes, J.E., Pinnegar, J.K., Moranta, J., 2001. Feeding relationships in Mediterranean bathyal assemblages elucidated by stable nitrogen and carbon isotope data. Mar. Ecol. Prog. Ser. 220: 13-23.

Pomeroy, L.R., 2001. Caught in the food web: complexity made simple? Sci. Mar. 65 (Suppl. 2): 31-40.

Portail, M., Olu, K., Dubois, S.F., Escobar-Briones, E., Gelinas, Y., Menot, L, Sarrazin, J., 2016. Food-Web Complexity in Guaymas Basin Hydrothermal Vents and Cold Seeps. PLoS ONE. 11(9): e0162263. DOI: 10.1371/journal.pone.0162263

Post, D.M., Pace, M.L., Hairston, N.G.J., 2000. Ecosystem size determines food chain length in lakes. Nature. 405: 1047-1049.

Post, D.M., 2002. Using stable isotopes to estimate trophic position: models, methods, and assumptions. Ecology. 83(3): 703-718.

Potier, M., Marsac, F., Cherel, Y., Lucas, V., Sabatié, R., Maury, O., Ménard, F., 2007. Forage fauna in the diet of three large pelagic fishes (lancetfish, swordfish and yellowfin tuna) in the western equatorial Indian Ocean. Fisheries Res. 83: 60-72. DOI: 10.1016/j.fishres.2006.08.020

Preciado, I., Cartes, J.E., Punzón, A., Frutos, I., López-López, L., Serrano, A., 2017. Food web functioning of the benthopelagic community in a deep-sea seamount based on diet and stable isotope analyses. Deep-Sea Res. II: 137: 56–68. https://doi.org/10.1016/j.dsr2.2016.07.013

Quartly, G.D., Buck, J.J.H., Srokosz, M.A., Coward, A.C., 2006. Eddies around Madagascar-The retroflection re-considered. J. Mar. Sci. 63: 115-129. DOI:10.1016/j.jmarsys.2006.06.001

Ramanantsoa, J. D., Krug, M., Penven, P., Rouault, M., Gula, J., 2018. Coastal upwelling south of Madagascar: Temporal and spatial variability. Journal of Marine Systems, 178: 29–37. https://doi.org/10.1016/j.jmarsys.2017.10.005

Reygondeau, G., Longhurst, A., Martinez, E., Beaugrand, G., Antoine, D., and Maury, O., 2013. Dynamic biogeochemical provinces in the global ocean. Global Biogeochemical Cycles, 27(4): 1046-1058. http://doi.org/10.1002/gbc.20089

Riley, G.A., 1971. Particulate organic matter in sea water. Advances in Marine Biology. 8: 1-118. https://doi.org/10.1016/S0065-2881(08)60491-5

Robison, B.H., 1984. Herbivory by the myctophid fish *Ceratoscopelus warmingii*. Mar. Biol. 84: 119-123.

Rogers, A.D., 1994. The biology of seamounts. In Advances in marine biology. Academic Press. 30: 305-350.

Romanov, E.V., 2003. Summary and review of Soviet and Ukrainian scientific and commercial fishing operations on the deep-water ridges of the southern Indian Ocean. (E. V Romanov, Ed.), FAO Fisheries Circular C991. Rome: FAO. http://www.fao.org/DOCREP/006/Y4884E/Y4884E00.HTM

Romero-Romero, S., Choy, C.A., Hannides, C.C.S., Popp, B.N., Drazen, J.C., 2019. Differences in the trophic ecology of micronekton driven by diel vertical migration. Limnol. Oceanogr. 1-11. DOI: 10.1002/lno.11128

Rubenstein, D.R., Hobson, K.A., 2004. From birds to butterflies: animal movement patterns and stable isotopes. Trends in Ecology and Evolution. 19(5): 256-263.

Ryan, C., McHugh, B., Trueman, C.N., Harrod, C., Berrow, S., O'Connor, I., 2012. Accounting for the effects of lipids in stable isotope ($\delta^{13}C$ and $\delta^{15}N$ values) analysis of skin and blubber of balaenopterid whales. Rapid Commun. Mass Spectrom. 26: 2745-2754. DOI: 10.1002/rcm.6394

Saino, T., Hattori, A., 1987. Geographical variation of the water column distribution of suspended particulate organic nitrogen and its ^{15}N natural abundance in the Pacific and its marginal seas. Deep-Sea Res. 34(5/6): 807-827.

Savoye, N., Aminot, A., Tréguer, P., Fontugne, M., Naulet, N., Kérouel, R., 2003. Dynamics of particulate organic matter $\delta^{15}N$ and $\delta^{13}C$ during spring phytoplankton blooms in a macrotidal ecosystem (Bay of Seine, France). Mar. Ecol. Prog. Ser. 255: 27-41.

Sholto-Douglas, A.D., Field, J.G., James, A.G., van der Merwe, N.J., 1991. $^{13}C/^{12}C$ and $^{15}N/^{14}N$ isotope ratios in the Southern Benguela Ecosystem: indicators of food web relationships among different size-classes of plankton and pelagic fish; differences between fish muscle and bone collagen tissues. Mar. Ecol. Prog. Ser. 78: 23-31.

Smith, M.M., Heemstra, P.C., 1986. Smith's Sea Fishes. J.L.B. Smith Institute of Ichthyology, Grahamstown, South Africa. 1047 p.

Sutton, T.T., 2013. Vertical ecology of the pelagic ocean: classical patterns and new perspectives. J. Fish. Biol. 83: 1508-1527. DOI: 10.1111/jfb.12263

Tanaka, H., Ohshimo, S., Sassa, C., & Aoki, I., 2007. Feeding habits of mesopelagic fishes off the coast of western Kyushu, Japan. PICES 16th: Bio, p-4200. 1st November.

Tew-Kai, E., Marsac, F., 2009. Patterns of variability of sea surface chlorophyll in the Mozambique Channel: a quantitative approach. J. Mar. Syst. 77 (1-2): 77-88. DOI: 10.1016/j.jmarsys.2008.11.007

Utrecht, W.L., van Utrecht-Cock, C.N., De Graaf, A.M.J., 1987. Growth and seasonal variations in distribution of *Chauliodus sloani* and *C. danae* (pisces) from the mid north atlantic. Bijdragen tot de Dierkunde. 57(2): 164-182.

Valls, M., Sweeting, C.J., Olivar, M.P., Fernández de Puelles, M.L., Pasqual, C., Polunin, N.V.C., Quetglas, A., 2014a. Structure and dynamics of food webs in the water column on shelf and slope grounds of the western Mediterranean. Journal of Marine Systems. 138: 171: 181. http://dx.doi.org/10.1016/j.jmarsys.2014.04.002

Valls, M., Olivar, M.P., Fernández de Puelles, M.L., Molí, B., Bernal, A., Sweeting, C.J., 2014b. Trophic structure of mesopelagic fishes in the western Mediterranean based on stable isotopes of carbon and nitrogen. Journal of Marine Systems. 138: 160-170. http://dx.doi.org/10.1016/j.jmarsys.2014.04.007

van der Spoel, S., Bleeker, J., 1991. Distribution of Myctophidae (Pisces, Myctophiformes) during the four seasons in the mid North Atlantic. Contributions to Zoology. 61(2): 89-106.

Vanderklift, M.A., Ponsard, S., 2003. Sources of variation in consumer-diet $\delta^{15}N$ enrichment: a meta-analysis. Oecologia. 136(2): 169-182.

Ventura, M., Catalan, J., 2008. Incorporating life histories and diet quality in stable isotope interpretations of crustacean zooplankton. Freshwater Biology. 53: 1453-1469. DOI: 10.1111/j.1365-2427.2008.01976.x

Vianello, P., Ternon, J-F., Herbette, S., Demarcq, H., Roberts, M.J., 2020. Circulation and hydrography in the vicinity of a shallow seamount on the northern Madagascar Ridge. Deep-Sea Res. II.

Vipin, P.M., Harikrishnan, M., Renju, R., Boopendranath, M.R., Remesan, M.P., 2018. Population Dynamics of Spinycheek Lanternfish *Benthosema fibulatum* (Gilbert and Cramer 1897), Caught off the South- west Coast of India. Asian Fisheries Science. 31: 161-171.

Waite, A.M., Muhling, B.A., Holl, C.M., Beckley, L.E., Montoya, J.P., Strzelecki, J., Thompson, P.A., Pesant, S., 2007. Food web structure in two counter-rotating eddies based on δ^{15}N and δ^{13}C isotopic analyses. Deep-Sea Res. II. 54: 1055-1075. DOI: 10.1016/j.dsr2.2006.12.010

Watanuki, Y., Thiebot, J-B., 2018. Factors affecting the importance of myctophids in the diet of the world's seabirds. Mar. Biol. 165: 79. https://doi.org/10.1007/s00227-018-3334-y

Young, J.W., Hunt, B.P.V., Cook, T.R., Llopiz, J.K., Hazen, E.L., Pethybridge, H.R., Ceccareli, D., Lorrain, A., Olson, R.J., Allain, V., Menkes, C., Patterson, T., Nicol, S., Lehodey, P., Kloser, R.J., Arrizabalaga, H., Choy, C.A., 2015. The trophodynamics of marine top predators: Current knowledge, recent advances and challenges. Deep Sea- Res. II. 113: 170-187. http://dx.doi.org/10.1016/j.dsr2.2014.05.015

List of tables and figures:

Table 1 Linear regression models fitted to $\delta^{15}N$ values (‰) with respect to body length in mm (SL, standard length for fish; TL, total length for leptocephali; ACL, abdomen and carapace length for the crustacean; DML, dorsal mantle length for the squid specimen) and the seamount variable (whether values were significantly different between La Pérouse and MAD-Ridge) of eight micronekton taxa- *Sigmops elongatus* (fish), *Ceratoscopelus warmingii* (fish), *Argyropelecus aculeatus* (fish), *Funchalia* sp. (crustacean), *Diaphus suborbitalis* (fish), *Abraliopsis* sp. (squid), *Chauliodus sloani* (fish), and leptocephali (fish).

Figure 1(a) Location of the MAD-Ridge and La Pérouse seamounts (black diamond symbols) in the East African Coastal (EAFR) and Indian South Subtropical Gyre (ISSG) provinces, respectively. Longhurst's (1998) biogeochemical provinces are delimited by black solid lines. Landmasses are shown in grey. Trawls #18-21 in the southern Mozambique Channel are shown by black stars and labelled "Trawl MZC". Map of (b) La Pérouse trawl stations numbered 1 to 10, (c) MAD-Ridge trawl stations numbered 1 to 17 plotted on the bathymetry (m). The colour bar indicates depth (m) below the sea surface.

Figure 2 Averaged satellite image of surface chlorophyll *a* concentrations from 18/09/2016 to 07/12/2016 at La Pérouse and MAD-Ridge (represented by black star symbols). The colour bar indicates the surface mean concentrations in mg m^{-3}. Monthly mean sea surface chlorophyll *a* concentrations (mg m^{-3}) from January to December 2016 for the regions defined by the red squares. The dates of the La Pérouse and MAD-Ridge cruises are marked by grey bars.

Figure 3. Bivariate plots of $\delta^{15}N$ and $\delta^{13}C$ values (‰) for particulate organic matter at the surface (POM-Surf) and the maximum fluorescence (POM-Fmax), zooplankton, gelatinous organisms, crustaceans, squid and mesopelagic fish sampled at La Pérouse and MAD-Ridge seamounts. Standard ellipse areas (coloured solid lines), calculated using SIBER, provide estimates of the size of the isotopic niche for each of these categories.

Figure 4. Boxplots of $\delta^{13}C$ and $\delta^{15}N$ values (‰) of the foodweb components POM-Surf, POM-Fmax, zooplankton (Zoopk), gelatinous organisms (Gel), crustaceans (Crust), squid and mesopelagic fish at La Pérouse (PER) and MAD-Ridge (MAD). Groups having significantly different $\delta^{13}C$ and $\delta^{15}N$ values (‰) are shown by solid blue lines.

Figure 5. $\delta^{15}N$ (mean ± S.D.) values (‰) and estimated trophic level (TL estimated from the TPA method) of POM-Surf, POM-Fmax, zooplankton, gelatinous and sampled micronekton species at the La Pérouse and MAD-Ridge seamounts. Taxa are placed in broad categories and $\delta^{15}N$ compositions are sorted in ascending order of their values.

Figure 6. Hierarchical clustering (Euclidean distance of normalised data subjected to averaged grouping) of $\delta^{13}C$ and $\delta^{15}N$ values (‰) of sampled gelatinous organisms, crustaceans, squid and mesopelagic fish at La Pérouse and MAD-Ridge. Roman numerals at the tree branches identify groups of species belonging to the different trophic guilds: group I – filter-feeders and detritivores; group II- omnivores and carnivores; subgroup IA: filter-feeders at La Pérouse and MAD-Ridge; subgroup IB: detritivores at both seamounts; subgroup IIA: filter-feeders and omnivorous crustaceans at La Pérouse, highest trophic level mesopelagic fish at MAD-Ridge; subgroups IIB: omnivorous and carnivorous micronekton at La Pérouse and MAD-Ridge.

Figure 7. δ^{15}N values (‰) of (a) fish: *Sigmops elongatus*, (b) fish: *Ceratoscopelus warmingii*, (c) fish: *Argyropelecus aculeatus*, (d) crustacean: *Funchalia* sp., (e) fish: *Diaphus suborbitalis*, (f) squid: *Abraliopsis* sp., (g) fish: *Chauliodus sloani*, (h) fish: leptocephali, plotted against size in mm [standard length for (a)-(c), (e), (g)-(h); abdomen and carapace length for (d); dorsal mantle length for (f)] at La Pérouse (squares) and MAD-Ridge (stars). Simple linear regressions for δ^{15}N values versus size are plotted for (a)-(d).

Figure 8(a) δ^{15}N values (‰) of mesopelagic fish from La Pérouse and MAD-Ridge seamount vicinities (LP_Vicinity and MR_Vicinity respectively) and from the Mozambique Channel, plotted against their standard lengths (mm). Simple linear regressions are plotted. (b) Bivariate plots of δ^{15}N and δ^{13}C values (‰) for selected seamount flank- and summit-associated fish species *D. suborbitalis* at La Pérouse (LP) and *B. fibulatum*, *D. knappi*, *C. japonicus* and *D. suborbitalis* at MAD-Ridge (MR) seamounts. Standard lengths are given in mm.

Figure 9. Boxplots of δ^{13}C and δ^{15}N values (‰) of omnivorous/carnivorous mesopelagic fish at La Pérouse flank (n = 50 samples) and vicinity (n = 60 samples) stations and, MAD-Ridge vicinity (n =91 samples), flank (n = 38 samples) and summit (n = 4 samples) stations, and stations from the southern Mozambique Channel (n = 28 samples). Outliers are shown as star symbols.

Table 1 Linear regression models fitted to $\delta^{15}N$ values (‰) with respect to body length in mm (SL, standard length for fishes; TL, total length for leptocephali larvae; ACL, abdomen and carapace length for the crustacean; DML, dorsal mantle length for the squid specimen) and the seamount variable (whether values were significantly different between La Pérouse and MAD-Ridge) of 8 micronekton taxa- *Sigmops elongatus* (fish), *Ceratoscopelus warmingii* (fish), *Argyropelecus aculeatus* (fish), *Funchalia* sp. (crustacean), *Diaphus suborbitalis* (fish), *Abraliopsis* sp. (squid), *Chauliodus sloani* (fish), and leptocephali (fish).

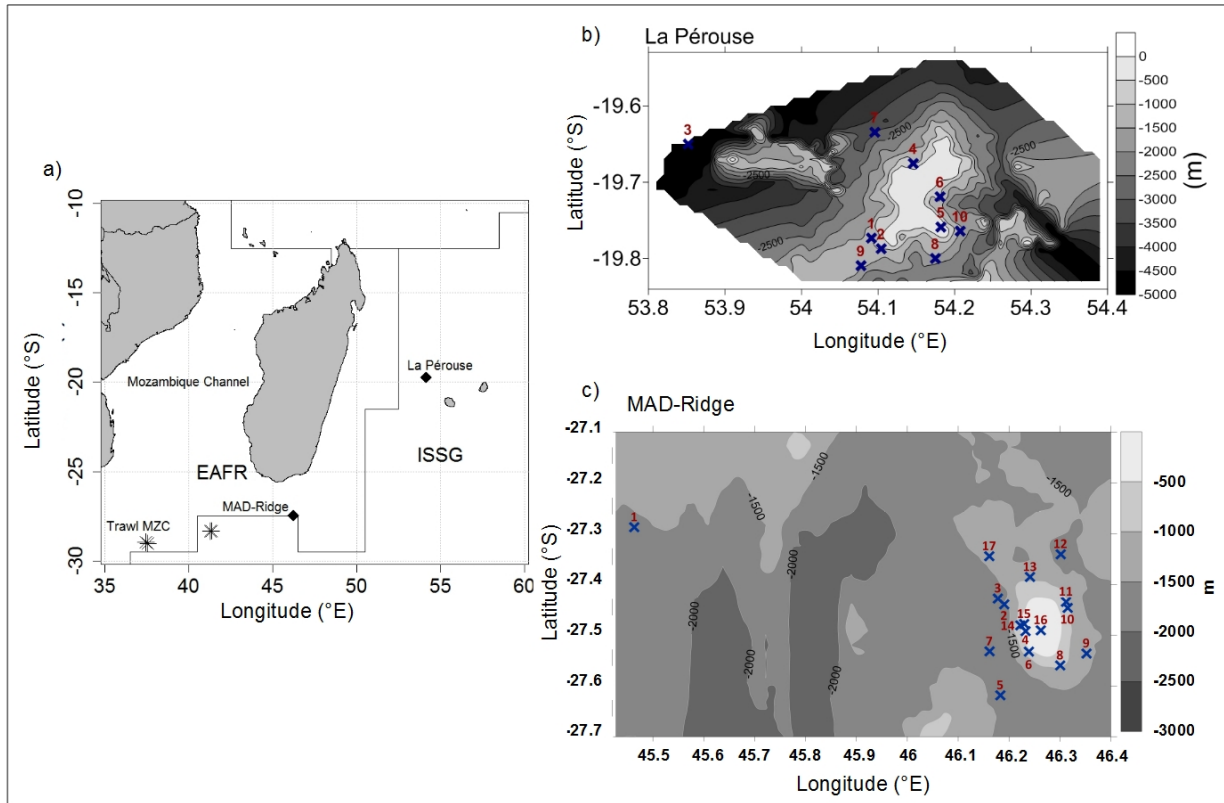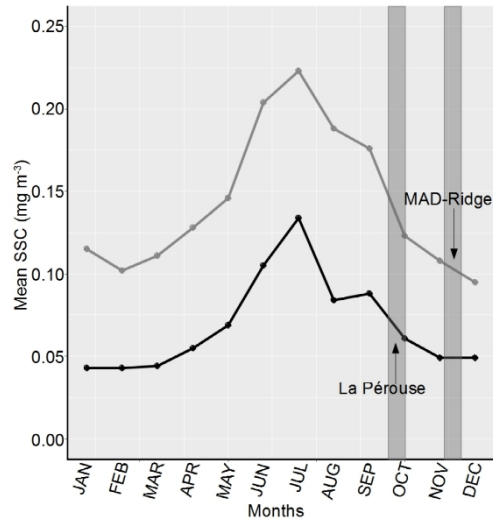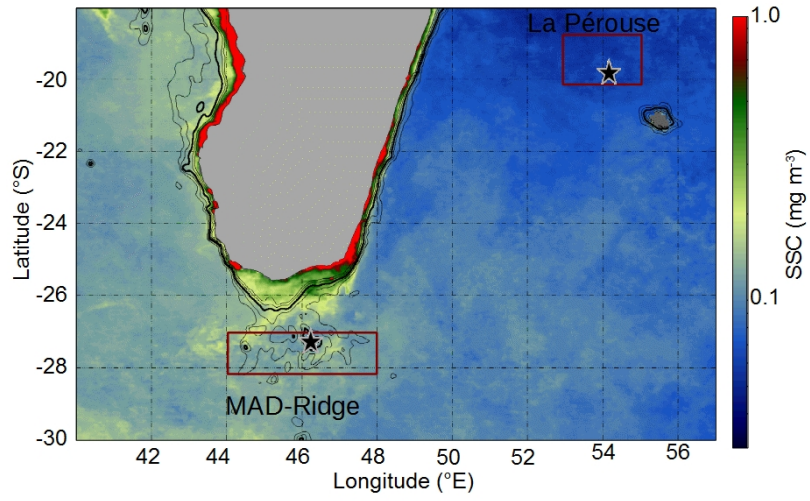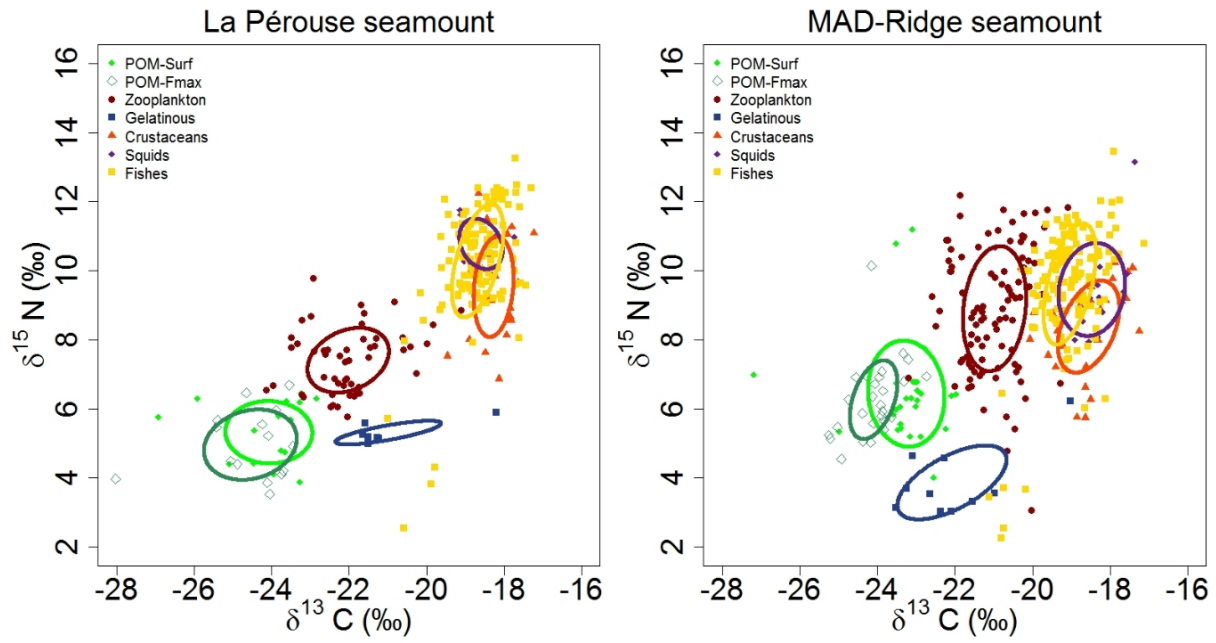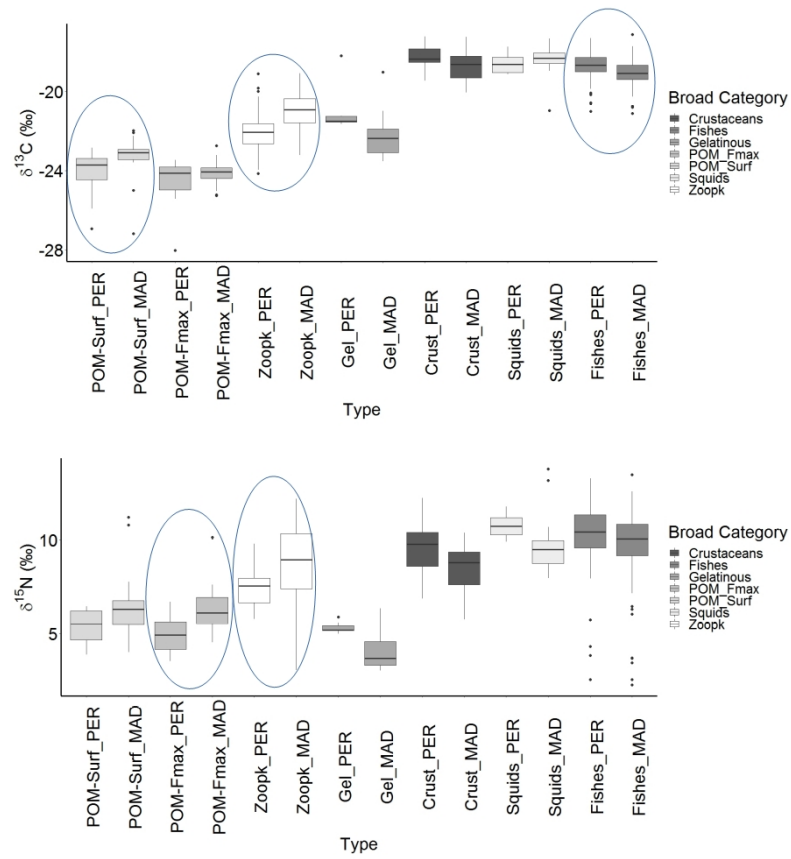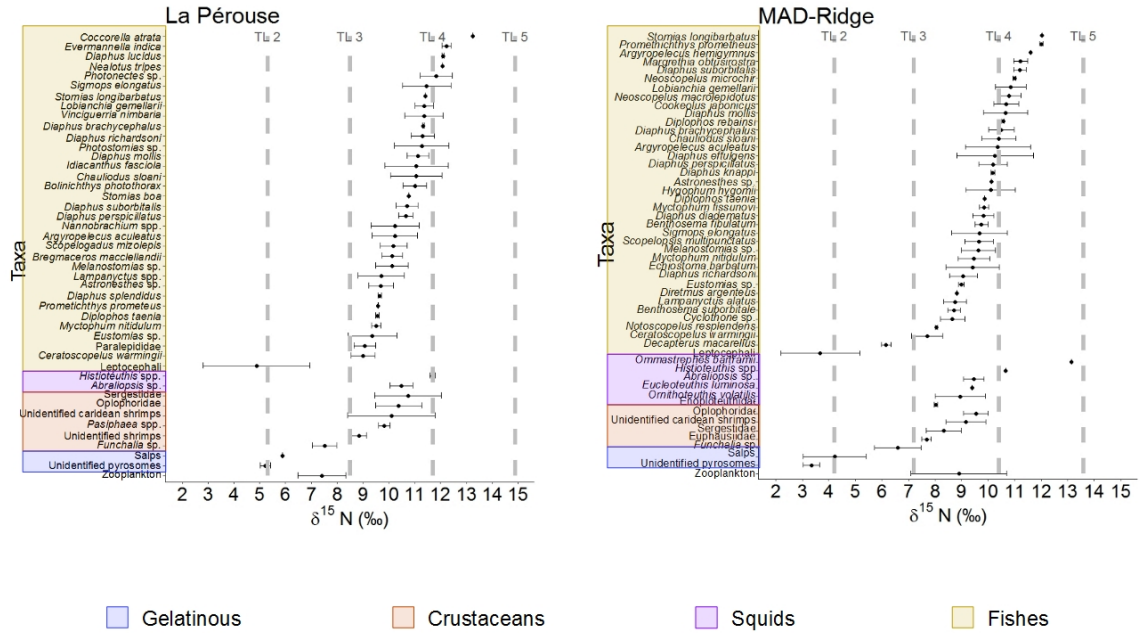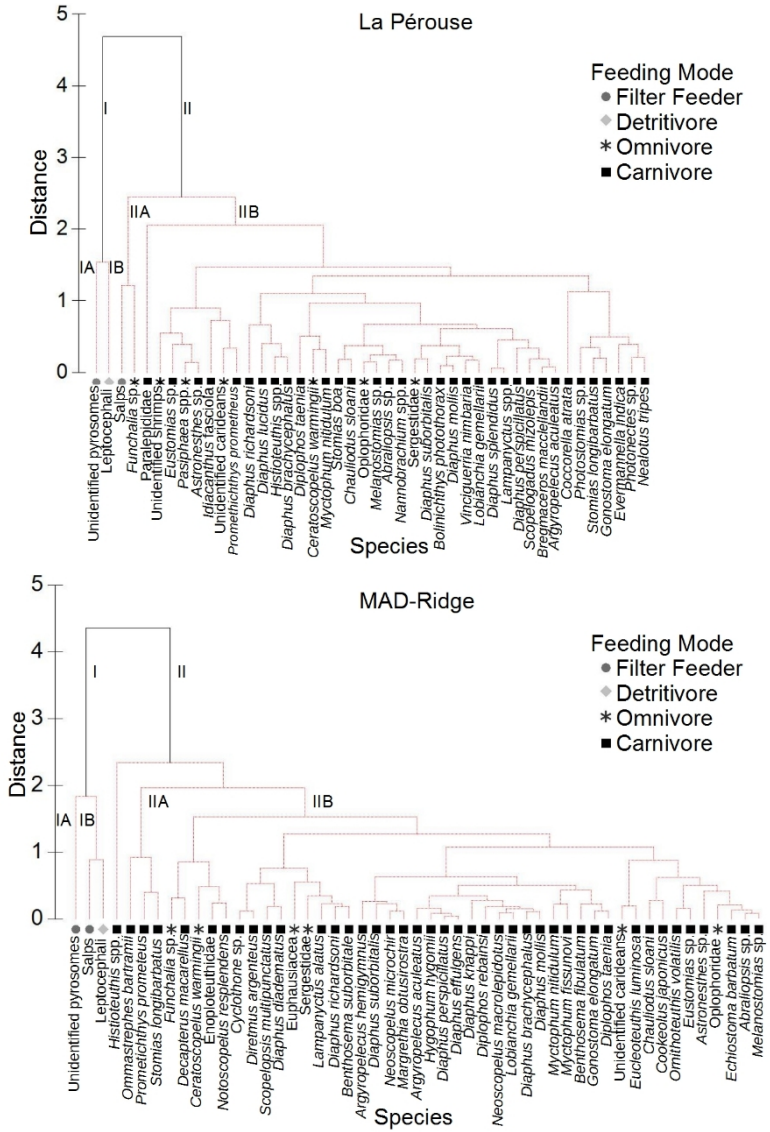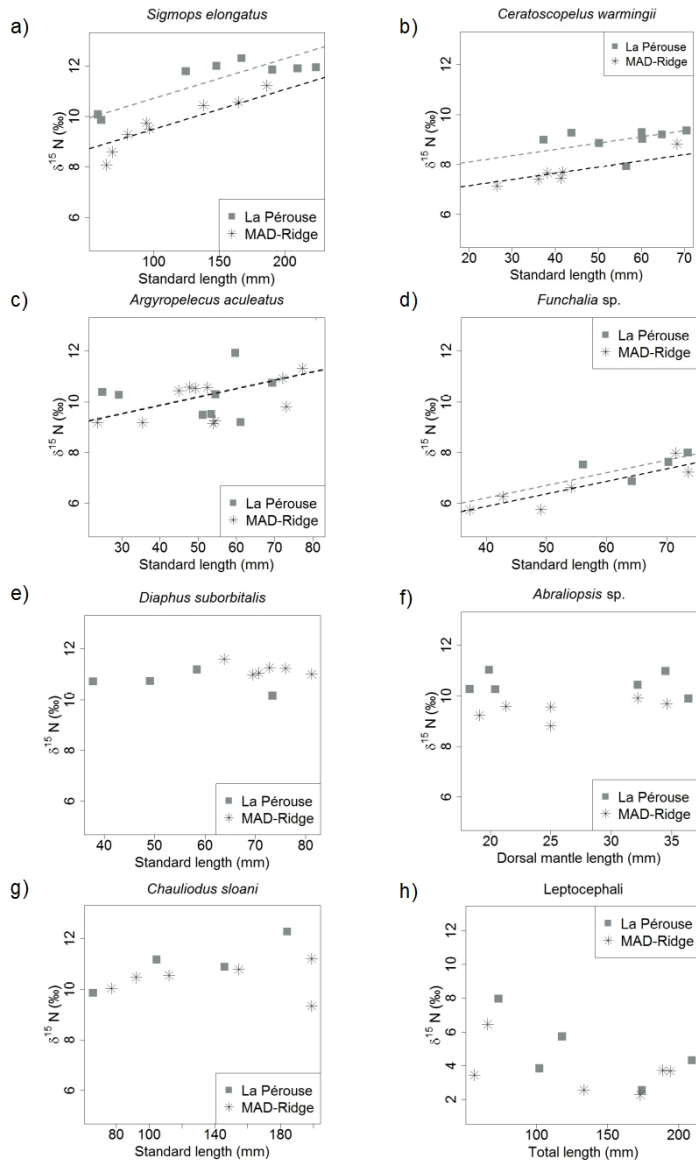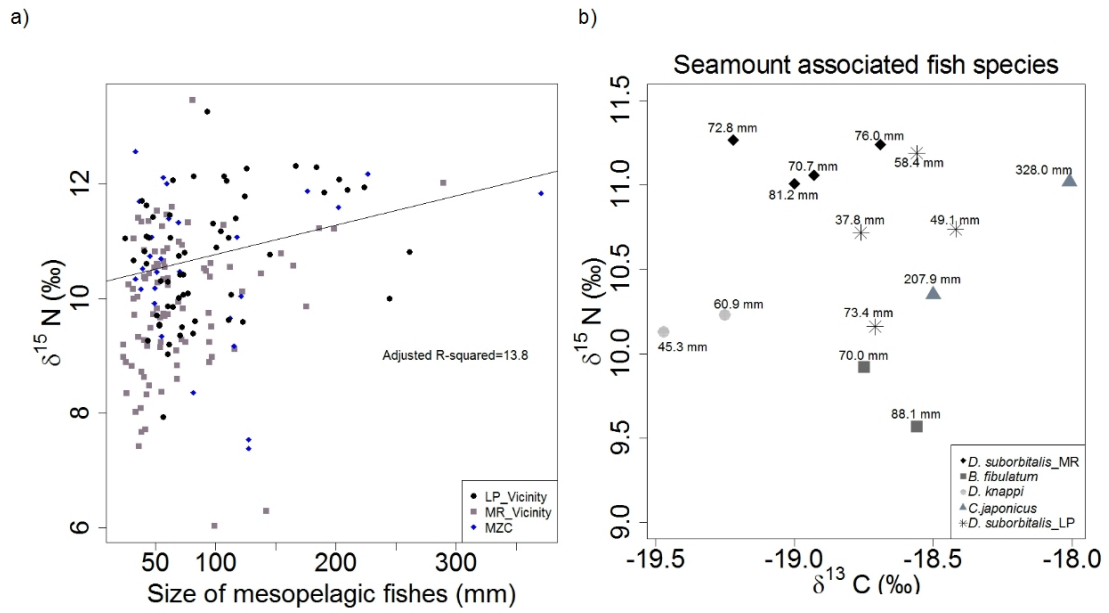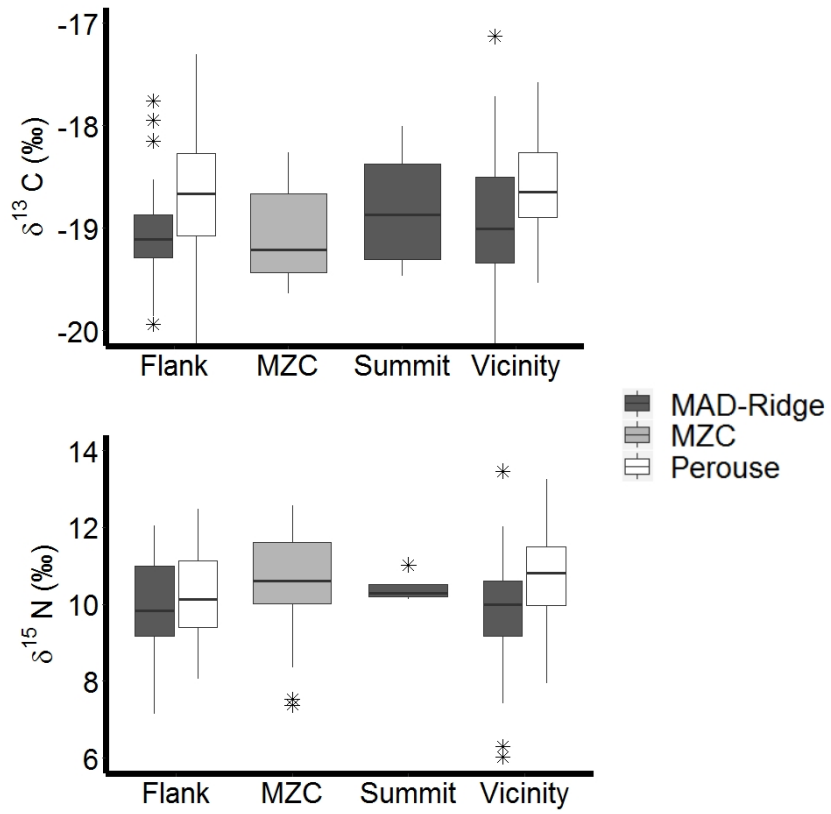| Taxon	Regression equation	Adjusted r^2 (%)	F-statistic	Degrees of freedom	P-value
Sigmops elongatus	$\delta^{15}N = 9.15 + 0.0157$ x SL $– 1.2210$ x seamount La Pérouse: $\delta^{15}N = 9.15 + 0.0157$ x SL MAD-Ridge: $\delta^{15}N = 7.93 + 0.0157$ x SL	85.2	46.0	13	< 0.05 for size and seamount
Ceratoscopelus warmingii	$\delta^{15}N = 7.61 + 0.0249$ x SL $- 0.9521$ x seamount La Pérouse: $\delta^{15}N = 7.61 + 0.0249$ x SL MAD-Ridge: $\delta^{15}N = 6.66 + 0.0249$ x SL	72.4	18.0	11	< 0.05 for size and seamount
Argyropelecus aculeatus	$\delta^{15}N = 8.57 + 0.0331$ x SL $- 0.0272$ x seamount	16.5	2.87	17	< 0.05 for size; > 0.05 for seamount
Funchalia sp.	$\delta^{15}N = 4.23 + 0.0496$ x ACL $- 0.3460$ x seamount	72.7	13.0	7	< 0.05 for size; > 0.05 for seamount
Diaphus suborbitalis	$\delta^{15}N = 11.5 - 0.0151$ x SL $+ 0.7594$ x seamount	43.8	4.51	7	> 0.05 for size; < 0.05 for seamount
Abraliopsis sp.	$\delta^{15}N = 10.3 + 0.0069$ x DML $- 1.006$ x seamount	56.2	8.06	9	> 0.05 for size; < 0.05 for seamount
Chauliodus sloani	$\delta^{15}N = 10.2 - 0.0065$ x SL $+ 0.7431$ x seamount	12.5	1.64	7	> 0.05 for size and seamount
Leptocephali larvae	$\delta^{15}N = 7.18 - 0.0170$ x TL $– 1.1971$ x seamount	25.3	2.69	8	> 0.05 for size and seamount

Figure 1

Figure 2

Figure 3

Figure 4

Figure 5

Figure 6

Figure 7

Figure 8

Figure 9